(delrapp.) 3128

VTT

Laboratory of Structural Engineering
Internal Report 19/1993

RAT-IR-19/1993

Heli Koukkari

LOADING TEST ON 265 MM HOLLOW CORE FLOOR WITH TOPPING SUPPORTED ON PRESTRESSED CONCRETE BEAM

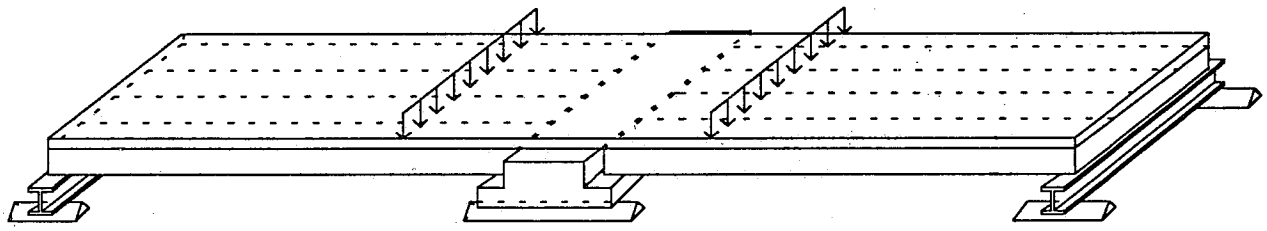

VTT RAKENNETEKNIIKAN LABORATORIO
LABORATORY OF STRUCTURAL ENGINEERING

Raporttikoodi - Report code	
RAT-IR-19/1993	
Päivväys - Date	*Projektinumero - Project number*
15.12.1993	RAT3563

Tekijät - Authors	*Projektin - nimi - Name of project*
Koukkari, Heli	Flexible Supports II
	Toimeksiantaja - Commissioned by
	Finnish Association of Building Industry RTT, the Int. Prestressed Hollow Core Association IPHA, KB Kristianstads Cementgjuteri, Sweden and Skanska Prefab AB, Sweden

Otsikko - Title
Loading test on 265 mm hollow core floor with topping supported on prestressed concrete beam

Päivitys raporttiin - Update to report	*Hyväksynyt - Approved by*
	J. Kuokkari
Julkisuus - Availability statement	*Määräpäivä - Until*
[ ] julkinen - public [x] luottamuksellinen - confidential	

Sarjan nimi - Series title	*Sivuja - Pages*
Laboratory of Structural Engineering, Internal Reports	30+ App. 41

Tiivistelmä - Abstract

VTT, Valtion teknillinen tutkimuskeskus
Rakennetekniikan laboratorio
Kemistintie 3, PL 26, 02151 Espoo
Puh. vaihde (90) 4561
Telekopio (90) 456 7003, teleksi 126022 vttth sf

VTT, Technical Research Centre of Finland
Laboratory of Structural Engineering
Kemistintie 3, P.O. Box 26, FIN - 02151 Espoo, FINLAND
Phone internat. +358 0 4561
Telefax + 358 0 456 7003, telex 126022 vttth sf

1 BACKGROUND

Since 1990, several full-scale loading tests on hollow core slabs supported on beams have been carried out in the Laboratory of Structural Engineering of the Technical Research Centre of Finland (VTT). Three separate tests were first carried out, financed by the Finnish companies Deltatek Oy and Rautaruukki Oy and the Association of the Concrete Industry of Finland.

After these tests a Nordic research project called "Shear capacity of hollow core slabs on flexible supports" was founded in order to develop new design rules. During this project three full-scale loading tests were carried out in 1991 - 1993. The Nordic project was financed by Lohja Oy, Finland, NCC Prefab AB, Sweden, Parma Oy, Finland, Oy Partek Concrete Ab, Finland, Skanska Prefab AB, Sweden and AB Strängbetong, Sweden. The Finnish companies were financially supported by the Technology Development Centre of Finland TEKES.

A design method for hollow core slabs supported on beams was proposed in the Nordic research program. The method is still in need of more accurate knowledge about the effects of different structural parts, e.g. topping with or without reinforcement, of the continuity and of the rigidity of the supporting beam. In order to improve the validity of the design method, new full-scale loading tests have been planned to be carried out during 1993 - 1994. At the moment, the financing bodies are the Finnish Association of Building Industry RTT, the International Prestressed Hollow Core Association IPHA, Kristianstads Cementgjuteri, Sweden, and Skanska Prefab AB, Sweden.

This report has been worked out by Heli Koukkari except Chapter 7 which has been written by Matti Pajari, who also planned the test.

2 ARRANGEMENTS OF THE FLOOR TEST

2.1 SPECIMENS AND LOADING ARRANGEMENT

An overview of the full-scale loading test is illustrated in Fig. 1. Eight hollow core slab units, each 265 mm in thickness and 6000 mm in length, were mounted on three simply supported beams from which the middle beam was a prestressed concrete beam and the edge beams were steel HE-beams. A reinforced concrete topping with a depth of 60 mm was cast over the whole floor. The floor was subjected to loading by two line loads placed parallel to the beams.

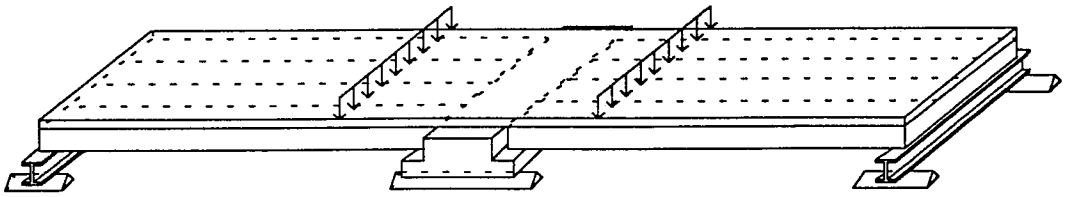

Fig. 1. Overview of the loading arrangement.

The first three above mentioned loading tests on 265 mm floors had shown that the shear failure of the hollow core units governs the load-carrying capacity of the floor. Therefore, the loading was arranged in order to clarify this failure mode. The following aspects were taken into account:

- The hollow core units should not fail in flexure. Therefore, the maximum number of prestressing strands (10 ϕ 12.5) was chosen and the line loads were located at a short distance (1000 mm) from the end of the slab units.
- The load-carrying capacity of the middle beam should be high enough to carry the load corresponding to the shear capacity of the slab calculated according to the conventional design method.
- The end beams were designed to deflect during the loading approximately as much as the middle beam. In this way, the torsion due to the different deflections between the ends beam and the middle could be minimized.
- The joints were similar to those used in practice.

The loads were introduced by eight actuators as shown in Fig. 2. The actuators no 1, 2, 3 and 4 were identical and connected to the same hydraulic circuit A. They were fixed in a permanent loading frame. The actuators no 5, 6, 7 and 8 were also identical and connected to another hydraulic circuit B. Their reaction forces were taken by an auxiliary frame. See also Figs 3 and 4 in App. 1.

The following notation is used:

P_1 Force in an actuator connected to the hydraulic circuit A
P_2 Force in an actuator connected to the hydraulic circuit B
F_1 Force (line load) on a hollow core unit due to P_1 and the weight of the loading equipment
F_2 Force (line load) on a hollow core unit due to P_2 and the weight of the loading equipment

The oil pressures in the hydraulic circuits A and B were manually controlled so that the actuator forces P_1 and P_2 were approximately equal. Taking into account the differences in the weight of the loading equipment, the following relationships can be written:

$$F_1 = P_1 + 1.2 \text{ kN}$$
$$F_2 = P_2 + 5.6 \text{ kN}$$

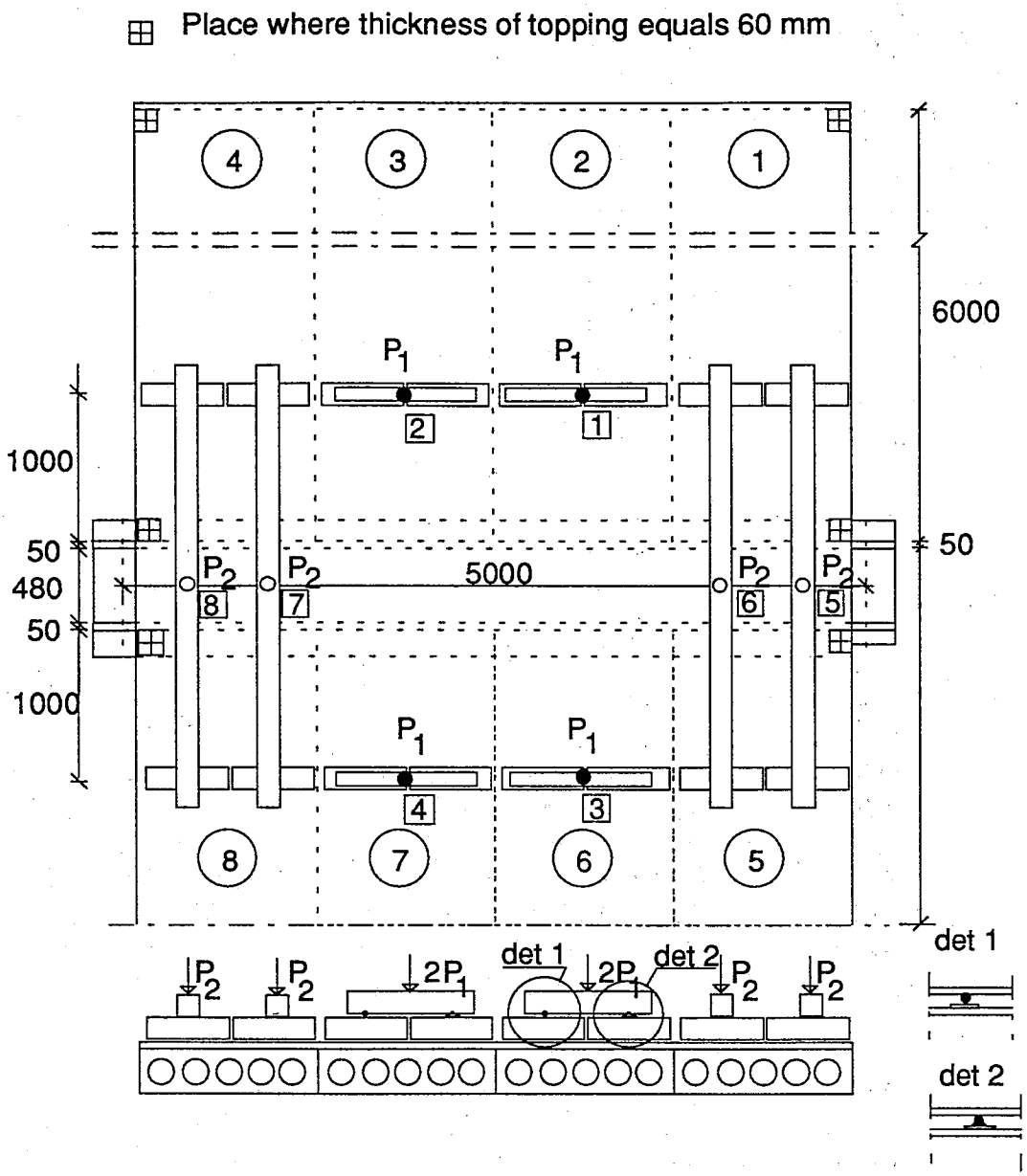

Fig. 2. Layout of the loading test.

The actuator forces were distributed into line loads on the slab units by means of 16 primary steel beams, each 550 mm in length. The surface of the concrete topping under these beams was evened by a thin gypsum layer. Secondary beams were laid on the primary spreader beams, in the circuit A parallel to the primary beams and in the circuit B perpendicular to the primary beams. The actuator forces were applied to the secondary beams.

Both ends of the actuators no 1, 2, 3 and 4 were provided with a swivel. Each secondary spreader beam under these actuators was freely supported on two

primary beams by means of a freely moving steel bar on a steel plate and a fixed steel bar on a steel plate placed in the middle of a primary beam (see also Fig. 2).

The contact between the actuators 5, 6, 7 and 8 and the secondary spreader beams was rigid (the lower end of an actuator) but there was a swivel between the upper end of the actuator and the auxiliary frame. The friction between the secondary and primary spreader beams was eliminated by teflon bearings consisting of two teflon sheets placed between the steel surfaces. The movement of the secondary beams in the perpendicular direction was prevented by L-shaped steel pieces welded to the primary beams (a small movement was possible). In the direction of the slab units, the movement of the secondary beams with respect to the primary beams was free, but the movement between the secondary beams and the auxiliary frame was prevented by the actuators.

2.2 SPECIMENS

2.2.1 Beams

The middle beam in the floor test was a prestressed concrete beam having a cross-section of an inverted T-beam. There were 18 prestressed tendons with a diameter of 12.5 mm and the initial prestress of 1100 MPa. The depth of the flange on which the hollow core units were supported was equal to 100 mm. The end beams were steel beams HE240. All the beams had a total length of 5200 mm. In Figs 3 and 4 the geometry of the middle beam and the end beams, respectively, is illustrated. More detailed drawings of the beams are shown in App. 2.

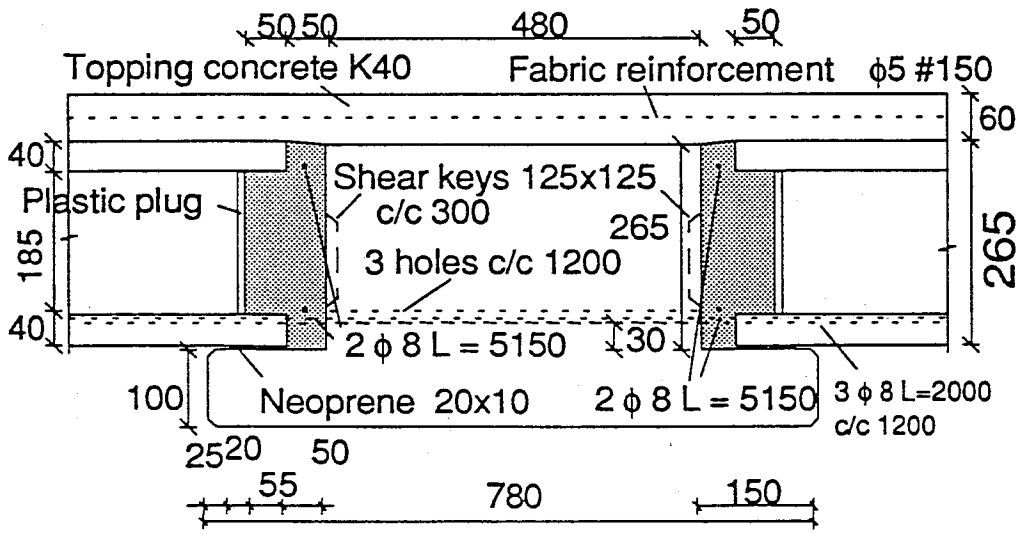

Fig. 3. The middle beam.

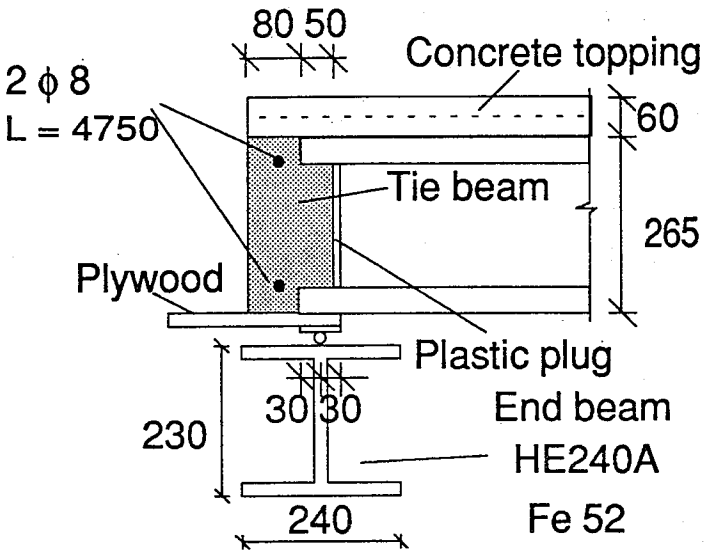

Fig. 4. The end beam.

2.2.2 Hollow core units

Ten hollow core units of the type VARIAX5 (five voids per unit) were made by Partek Concrete Oy in Hyrylä on 15th of September 1993. They were nominally 265 mm in thickness and 6000 mm in length. Each unit was prestressed with 10 strands, each 12.5 mm in diameter. The initial prestress was equal to 950 MPa. The units no 1 - 8 were used in the floor test and the unit no 9 was used in the reference tests. The slab unit no 10 was for safety, and it was taken from an other casting bed than the slab units no 1 - 9. The nominal and measured cross-sectional geometry of all the slab units is given in App. 3.

2.3 SPECIMEN ASSEMBLING

The beams were first installed on their supports (see also Figs 1 and 2 in App. 1). The hollow core units, the reinforcement in the tie beams and the reinforcement in the joints were then placed (see also Figs 3 and 4). Thereafter, the joints and the tie beams were concreted on the 24th of September, 1993. The mesh reinforcement over the whole floor was placed (see also Fig. 23 in App. 1 and App. 2). The topping concrete was cast on the 29th of September. The top surfaces of the slab units and of the beam were cleaned and moistened. No special measures were taken in order to enhance the bond between the topping and the prefabricated members.

No temporary supports were used under the beams.

2.4 MEASUREMENTS IN THE LOADING TEST

2.4.1 Vertical displacements

The deflection of the floor (vertical displacements) was measured by inductive transducers on the top of the floor specimen at five lines I - V as shown in Fig. 5.

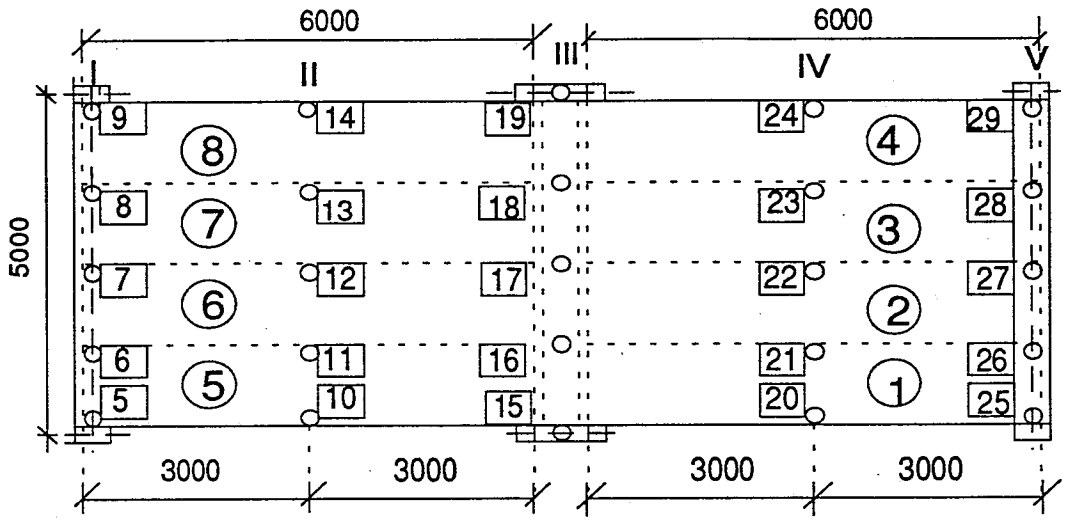

Fig. 5. Location (small circle) and numbering (small rectangular) of transducers for measuring vertical displacement.

2.4.2 Horizontal displacement

The horizontal displacement differences between different structural parts were measured at points shown in Figs. 6 and 7.

The transducers no 40 - 45 measured the width of a possible crack developing in the concrete topping over the joint between the slab units and the middle beam.

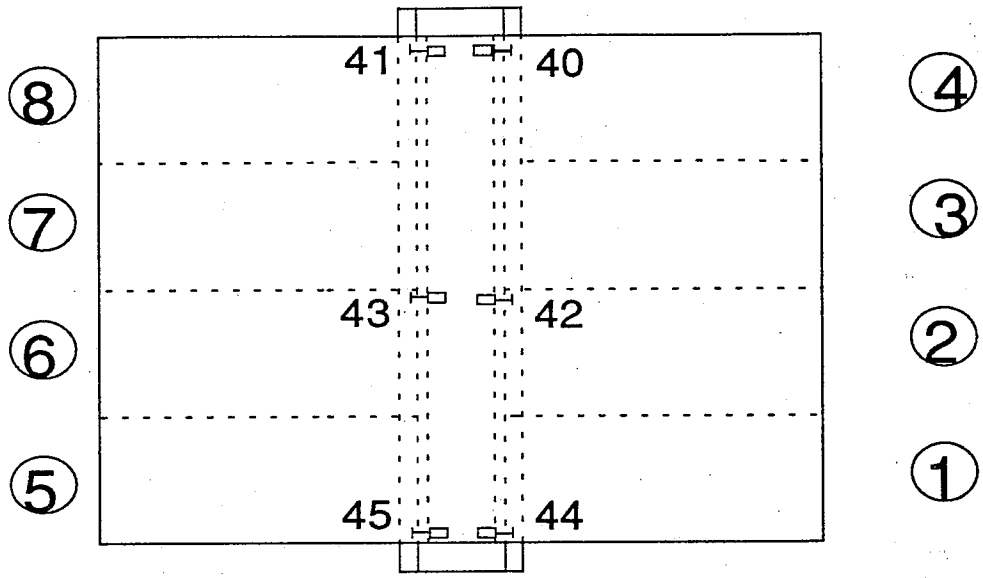

Fig. 6. Location of transducers no 40 - 45.

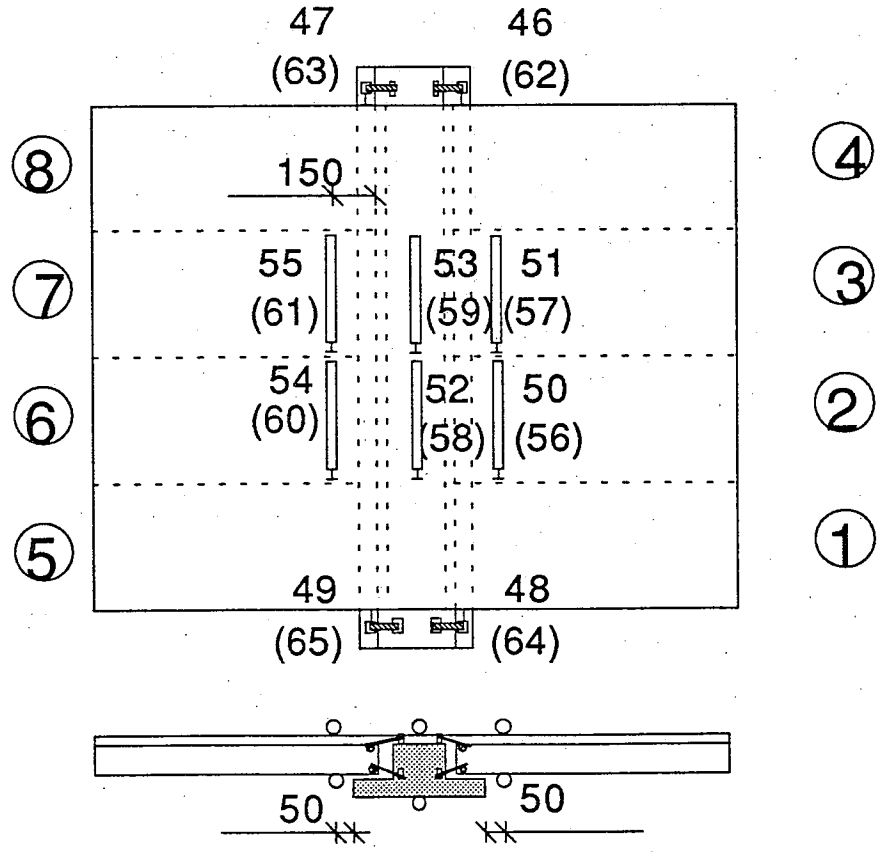

Fig. 7. Location of transducers no 46 - 65 for measuring horizontal displacement difference. The numbers in parentheses refer to the transducers at the bottom of the floor.

The transducers no 50 - 61 measured the possible differences in displacements parallel to the beam between the edges of the hollow core units and corresponding points on the middle beam. The transducers no 50 - 55 were located on the concrete topping. See also Figs 5 and 6 in App. 1.

The transducers no 46 - 49 and 62 - 65 measured the displacement differences between the beam and the edge of the hollow core slab in the direction of the beam (see also Fig. 7 in App. 1).

2.4.3 Force measurement

The actuator forces were measured by means of load cells. The support reaction under one support of the middle beam was measured by three load cells as shown in Fig. 8.

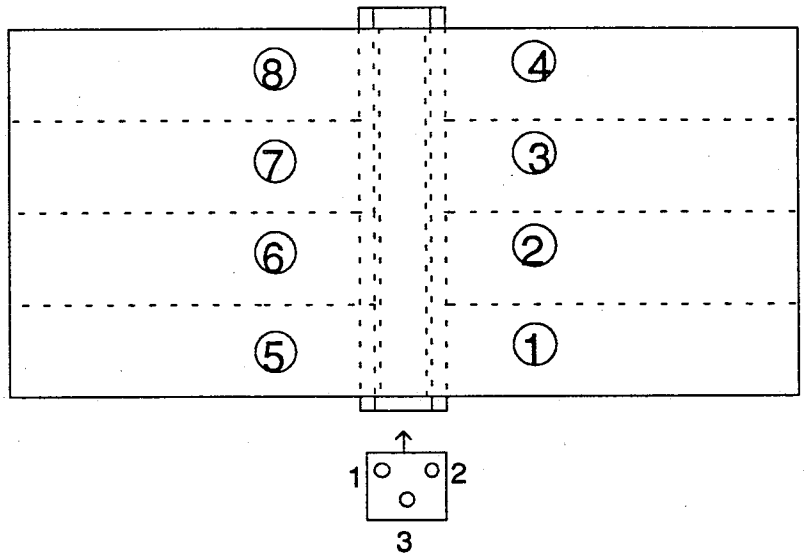

Fig. 8. Load cells under the support of the middle beam.

3 FLOOR TEST

3.1 LOADING HISTORY

The date of the loading test was 11th of October, 1993.

All the measuring devices were zero balanced when the actuator forces P_1 and P_2 were equal to zero while the weight of the loading equipment and the self weight of the structure were applied.

The floor was first loaded cyclically. The actuator forces were increased five times to $P_1 = P_2 = 55$ kN and then reduced back to zero. Thereafter the loading was increased monotonously to failure. The observations of the development of the cracking are presented also in Table 1.

Under the forces $P_i = 55$ kN in the first cycle, vertical cracks could be seen on the upper corner of a flange of the concrete beam, under the slab no 6. One vertical crack on both longitudinal edges of the concrete topping was also induced at or near the vertical joint between the slabs and the middle beam, and these cracks reached about 200 mm on the surface of the topping near the slabs no 4 and 5. A vertical crack developed in the middle of both concrete edge beams cast over the steel beams, between the slabs no 2 and 3, and no 6 and 7.

Under the forces $P_i = 55$ kN in the third cycle several vertical cracks developed at both ends of the concrete middle beam and they extended also to the beam surface. In the fifth cycle a new vertical crack formed in the longitudinal edge of the concrete topping near the slab no 1. See also Figs. 8 - 13 in App. 1.

When the loads were again increased after the cycles, under the forces $P_i = 60$ kN, vertical cracks in the flange edge of the middle beam grew down to the bottom surface.

Cracks appeared on the surface of the topping along the joint between the middle beam and the ends of the slabs no 1 - 4, when the forces $P_i = 80$ kN, and a transverse crack developed on the bottom of the middle beam. At the forces $P_i = 90$ kN the cracks in the middle of the edge tie beams reached the surface of the topping and a diagonal crack starting from the corner of the middle beam formed in the edge of the topping above the slab no 4.

At the forces $P_i = 100$ kN, a vertical crack developed in the concrete tie beam, between the slabs no 5 and 6, and a vertical crack induced in the joint between the slab no 1 and the middle beam next to the beam.

In the joint between the middle beam and the slab no 5 a crack developed next to the beam, under the forces $P_i = 110$ kN. Under the forces $P_i = 115$ kN a vertical crack developed in the edge of the topping starting from the corner of the middle beam near the slab no 1 and at the same time the concrete topping was loose above the beam end between the slabs no 1 and 5.

Table 1. Observations on the cracking during the loading test.

P_i kN	OBSERVATIONS	CRACKING PATTERN
55 (1)	Vertical cracks in the flange of the middle beam, under the slab unit no 6	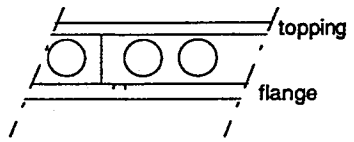
55 (1)	Vertical cracks in the longitudinal edges of the topping, above the middle beam ends	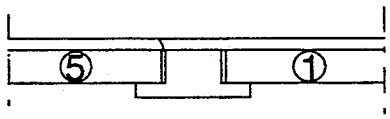
55(1)	One vertical crack in the edge tie beam, above the HE-beam	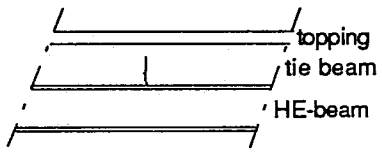
55(3)	Several vertical cracks in the middle beam ends	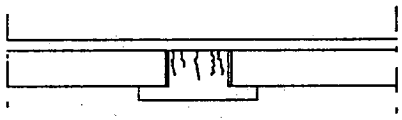
55(5)	A vertical crack in the longitudinal edge of the topping	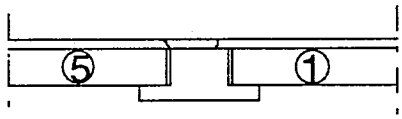
60	Cracking in the middle beam flange grew down to the bottom of the beam	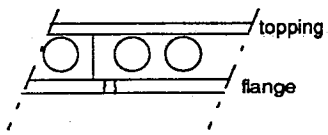
80	Cracks formed on the surface of the topping along the joint between the middle beam and the slabs no 1 - 4	see Fig. 9

Table 1. Continued.

80	A transverse crack on the bottom of the middle beam	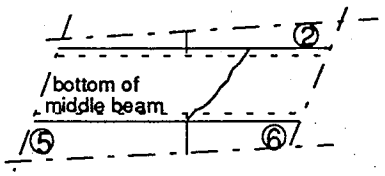
90	The cracks in the edge tie beams reached the surface ot the topping	
90	A vertical crack formed in the longitudinal edge of the topping starting from the corner of the middle beam	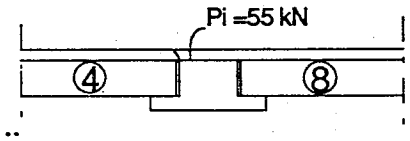
100	A vertical crack developed in the concrete tie beam, between the slab units no 5 and 6	
100	A vertical crack formed in the joint between the slab unit no 1 and the middle beam, next to the beam	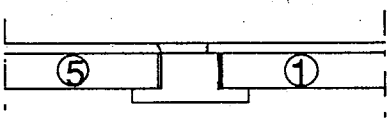
110	A vertical crack developed in the joint between the slab unit no 5 and the middle beam, next to the beam	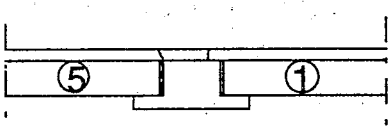
115	A vertical crack developed in the longitudinal edge of the topping starting from the corner of the middle beam	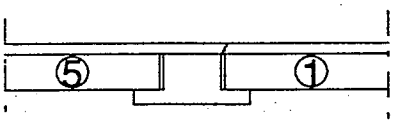
115	The concrete topping became loose above the middle beam, between the slab units no 1 and 5	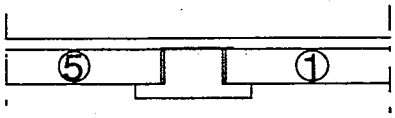

Diagonal cracks developed in the edges of the slabs no 1 and 4 near the middle beam under the forces P_i = 120 kN and a crack along the joint between the middle beam and the slabs no 5 - 8 developed in the surface of the topping (see Fig. 9 and also Figs. 10 and 12 in App. 1). After a while diagonal cracks appeared in the slabs no 5 and 8 (see Figs. 11 and 13 in App. 1). New diagonal cracks developed on all the slab edges near the middle beam, when the forces were increased until the failure under the forces P_i = 135 kN.

The shear forces caused the failure of the floor. The cracking patterns after the failure are shown in Fig. 9 and in App. 1 (Figs. 14 - 18).

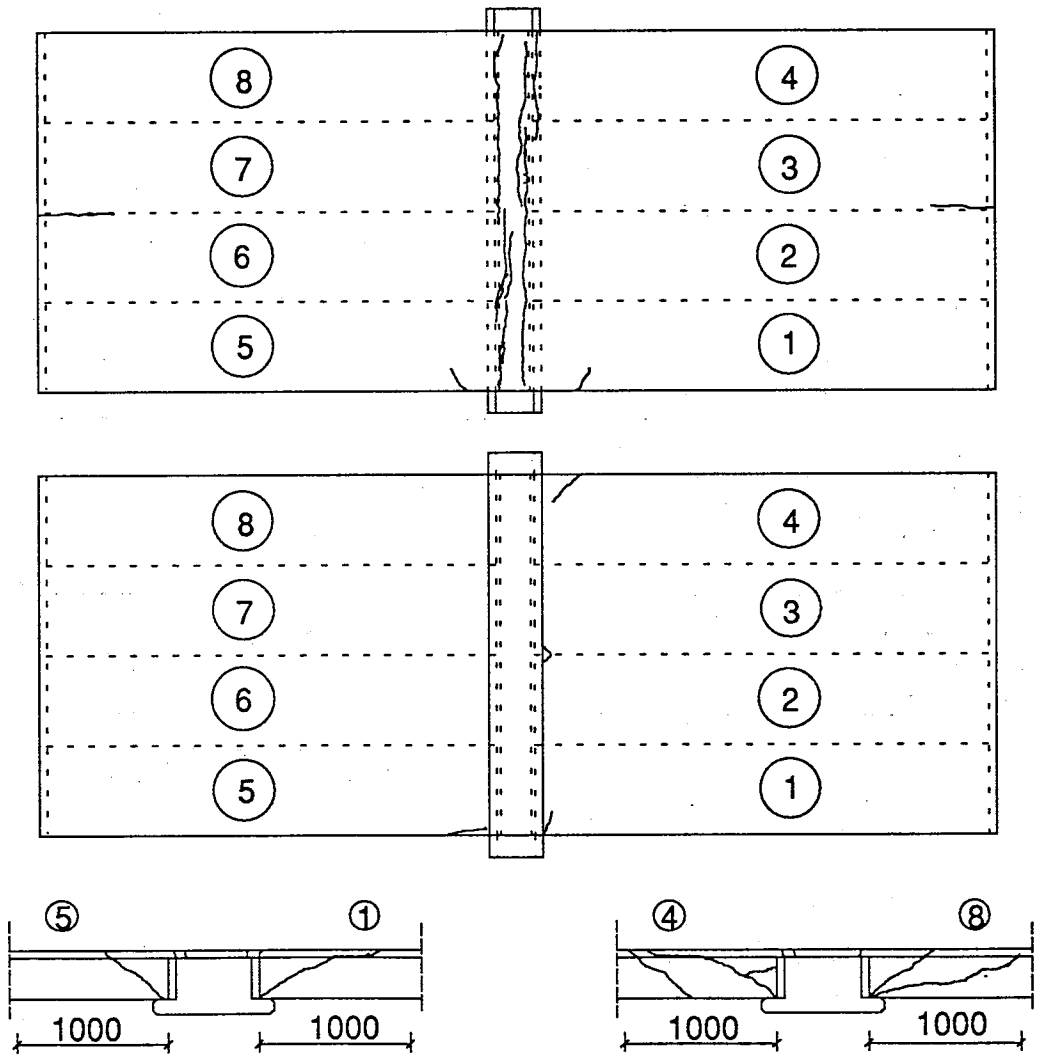

Fig. 9. Cracking pattern at the surface of the topping, at the bottom of the test floor and at the longitudinal edges of the floor after failure.

The loading test took 3.5 hours.

3.2 DEFLECTION

Due to the nature of the studied problem, the deformation of the middle beam and that of the hollow core units is of main interest, not the rigid body motion caused by the yielding of the supports of the beam. Therefore, the vertical displacements of the middle beam have been eliminated from all the load - deflection curves presented in this section. On the other hand, the possible yielding of the end beam supports has not been taken into account. The elimination method is clarified in App. 4. The displacements measured from the original position are given in tables in App. 5.

The load- deflection relationship for the midpoint of the middle beam is illustrated in Fig. 10.

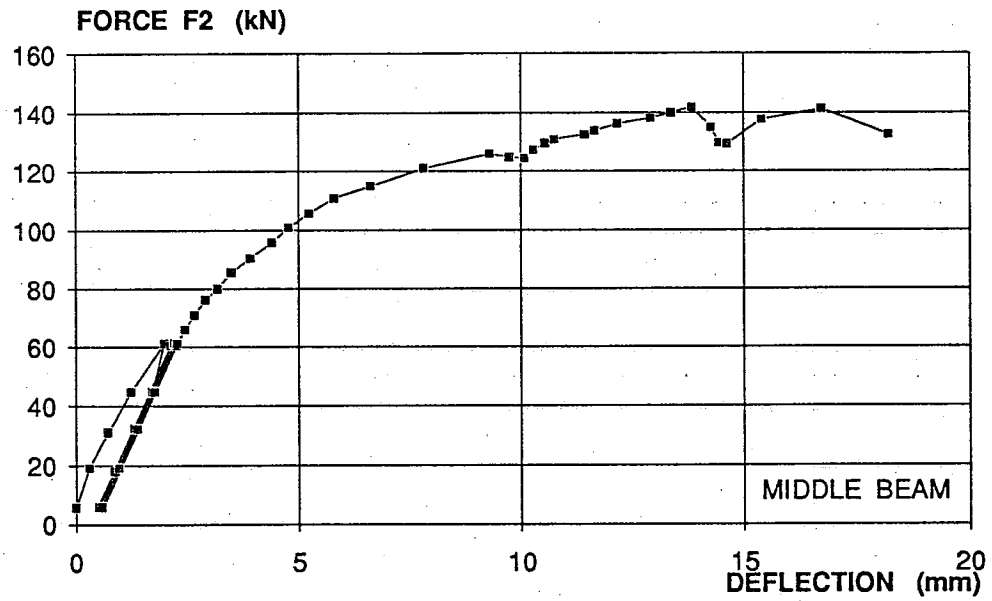

Fig. 10. Midpoint deflection of the middle beam.

The deflections of all measure points are illustrated in Figs 11- 15. In these figures F2 denotes the line load F_2 on one slab unit and it includes both the weight of the loading equipment and the load caused by the hydraulic actuator. The numerical values for the forces F_1 and F_2 and for the deflections as measured from the original point are presented in App. 5.

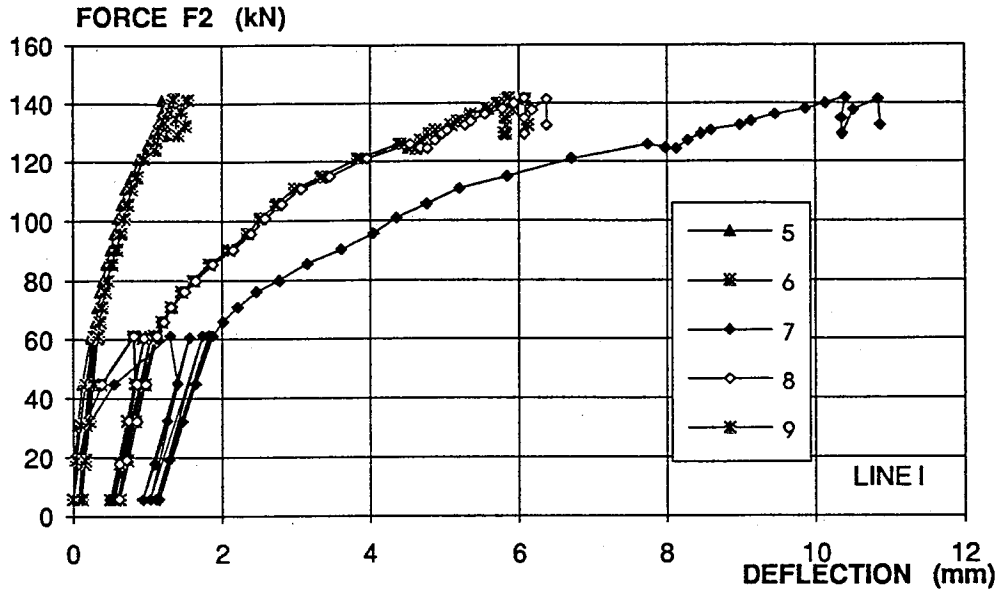

Fig. 11. Deflections at line I.

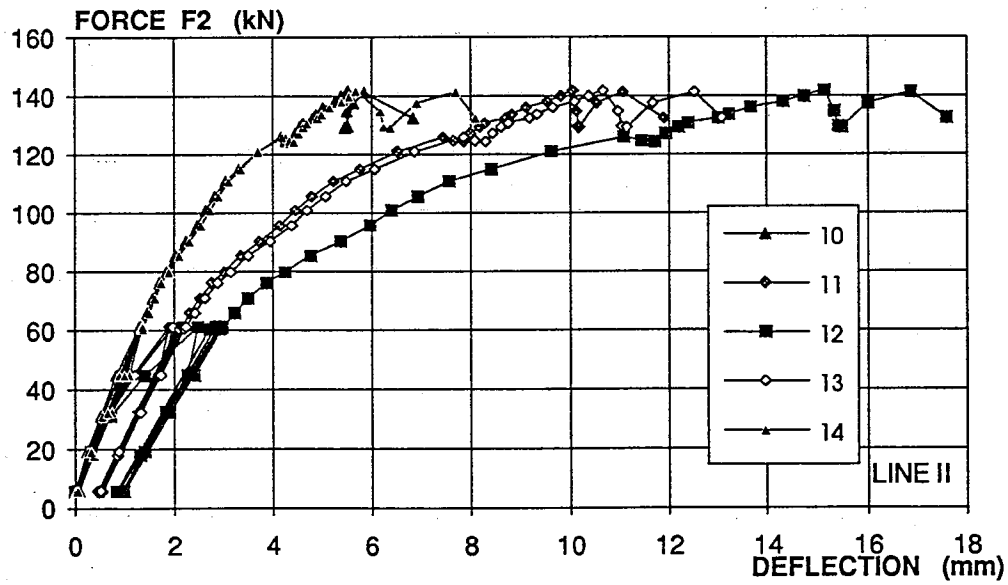

Fig. 12. Deflections at line II.

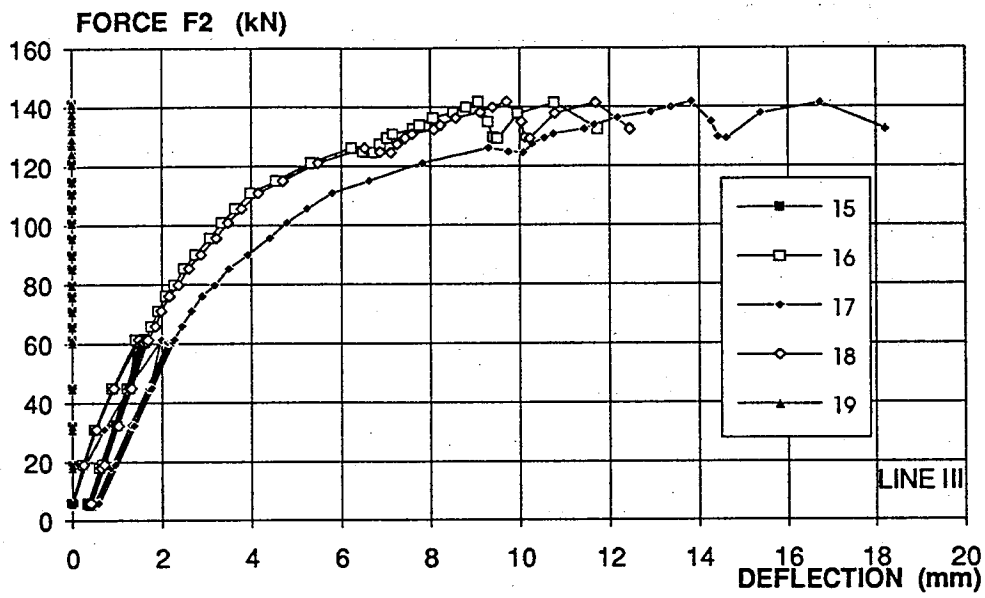

Fig. 13. Deflections at line III.

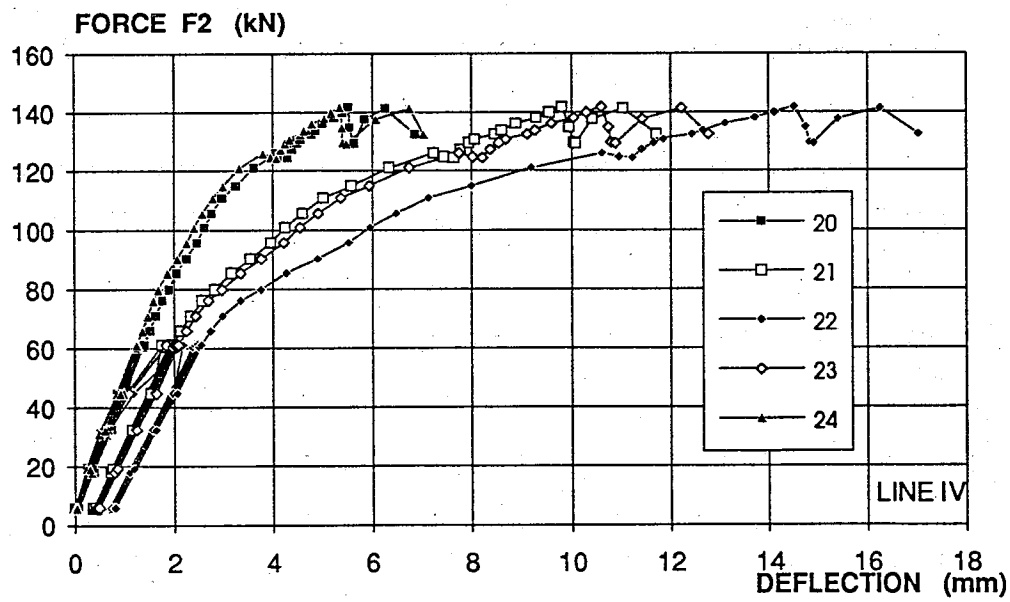

Fig. 14. Deflections at line IV.

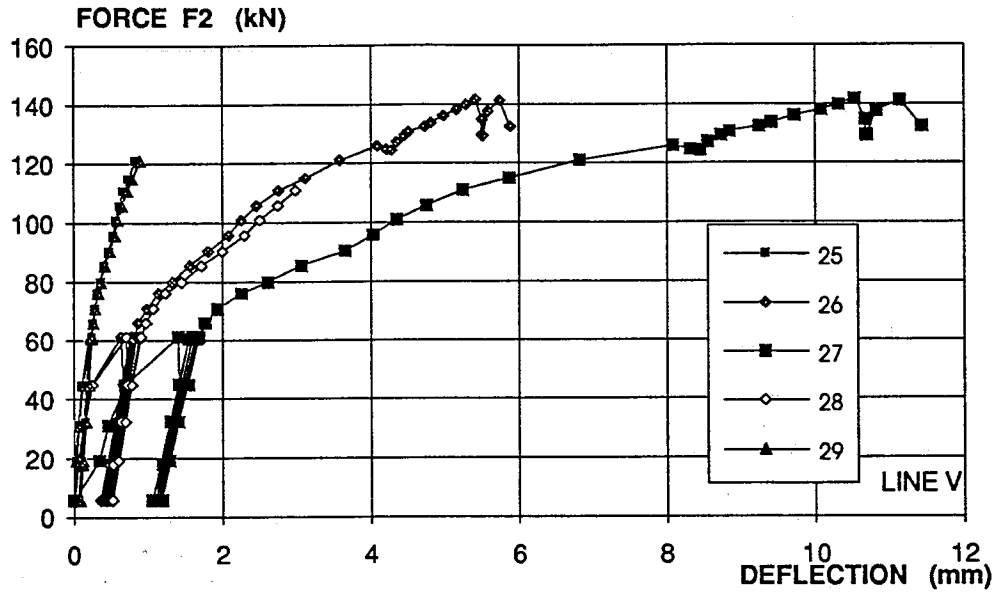

Fig. 15. Deflections at line V.

The measuring devices were mechanically disturbed during the test at points 25, 28 and 29, and for this reason the curves for these points are cut in Fig. 15.

3.3 REACTION FORCE UNDER THE MIDDLE BEAM AND THE OBSERVED SHEAR CAPACITY OF A HOLLOW CORE SLAB

In Fig. 16 the reaction force measured under one end of the middle beam is shown as a function of the load on a half floor ($=2(F_1+F_2)$). The relationship is almost linear until failure and shows that the measured support reaction of the middle beam is about 88.3% of the line load. It is greater than the calculated value of the support reaction assuming that the slabs are simply supported on the beams which is 84 %. This difference is due to the reinforced concrete topping which caused a negative bending moment at the middle beam.

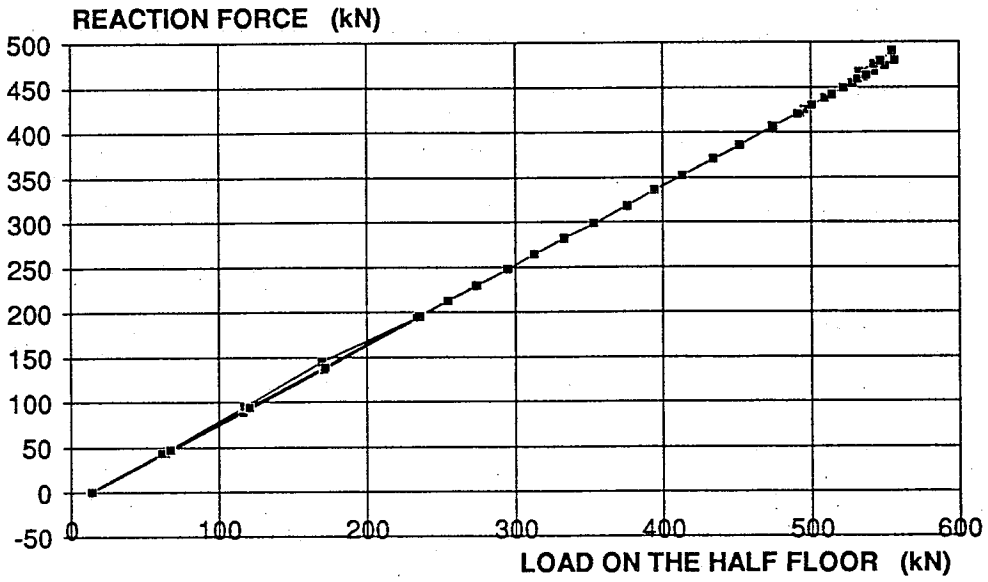

Fig. 16. Reaction force under one end of the middle beam.

From the relation of the reaction force to the load on the half floor, it is possible to calculate that the support reaction of the hollow core unit 1 or 4 due to imposed load was equal to

$$V_{u,imp} = 0.883 \cdot 2 \cdot (F_1+F_2)/4 = 0.883 \cdot 556.8 \text{ kN}/4 = 122.9 \text{ kN}$$

at failure. Using the measured weight of the slab units (see App. 3), the support reaction due to the weight of the jointed slab unit $V_{u,gs}$ = 12.6 kN is obtained. Similarly, the weight of the concrete topping caused the support reaction $V_{u,gt}$ = 4.7 kN. Hence the observed ultimate shear capacity (support reaction) is given by

$$V_u = 122.9 \text{ kN} + 12.6 \text{ kN} + 4.7 \text{ kN} = 140.2 \text{ kN}.$$

3.4 DISPLACEMENT DIFFERENCES BETWEEN THE ENDS OF THE MIDDLE BEAM AND SLAB EDGES

The curves for measured displacement differences between the edges of the slab units and the middle beam are presented in Figs. 17 and 18.

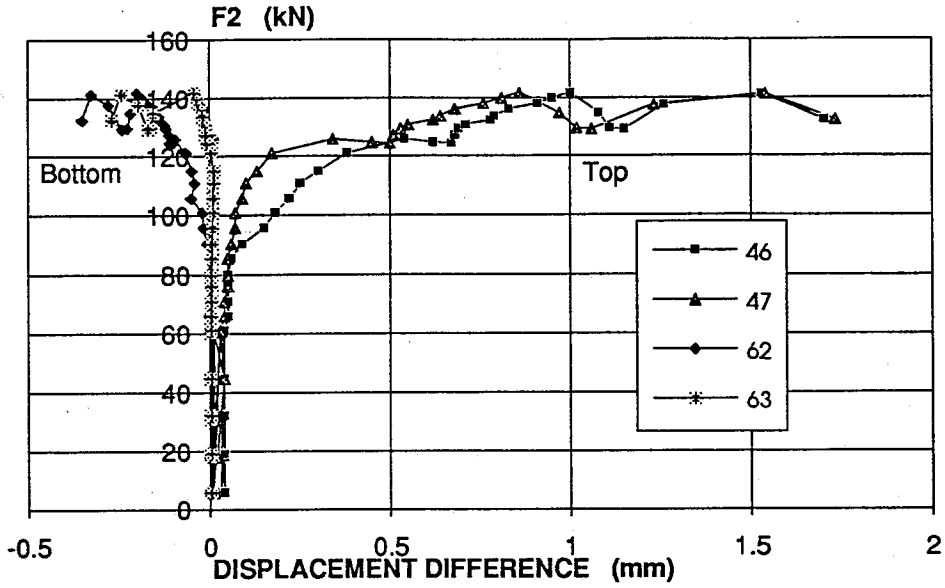

Fig. 17. Displacement difference between the end of the middle beam and the edges of slabs no 4 and 8.

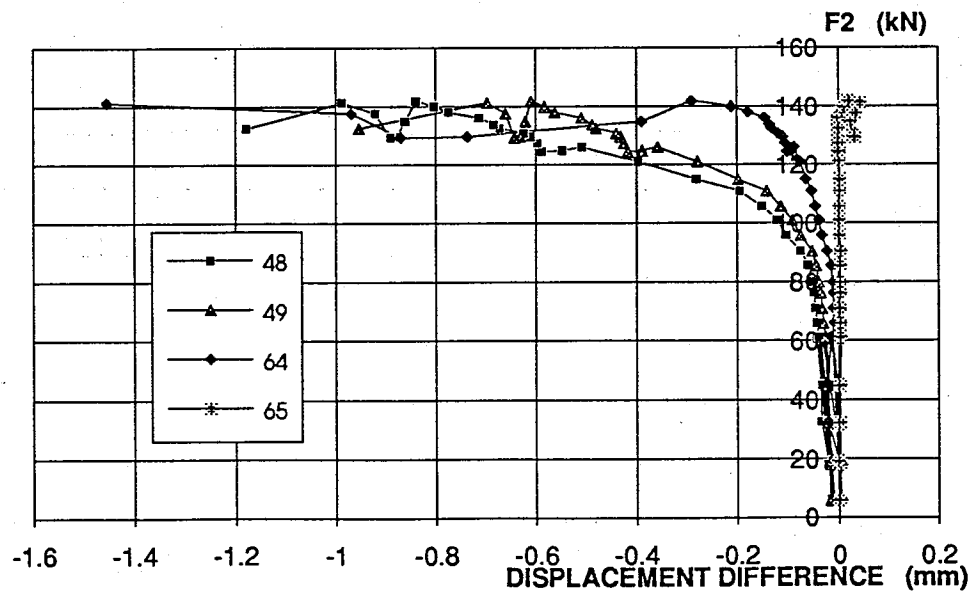

Fig. 18. Displacement difference between the end of the middle beam and the edges of slabs no 1 and 5. A negative sign means that the measurement points became closer to each other.

According to Fig. 17 the displacement of the top flanges of the hollow core units no 4 and 8 relative to the beam has been positive, i.e. the slab edge moved further compared to the upper measurement point of the middle beam. No explanation can be given for these unexpected results.

3.5 CRACK WIDTH OVER THE VERTICAL JOINTS

The crack width (the sum of the crack widths) in the concrete topping just over the vertical joints between the slab units and the middle beam is shown in Fig. 19.

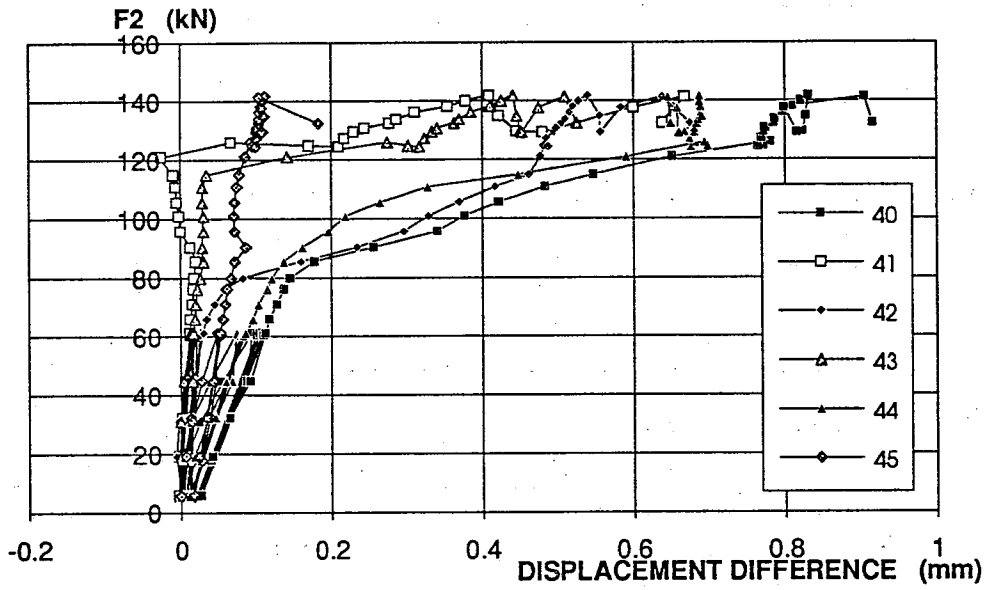

Fig. 19. The sums of the crack widths in the concrete topping over the vertical joints adjacent to the middle beam.

The measurements at the points no 40, 42 and 44 show the same kind of a behaviour as observed visually: under the forces P_i = 80 kN a crack formed along the joint between the ends of the slab units no 1 - 4 and the middle beam. It can also be seen from the results at the points no 41 and 43, that under the forces P_i = 120 kN a crack developed along the other side of the middle beam. The exact location of the cracks were different from the location of the joints (see also Figs 14, 15 and 16 in App. 1). Therefore, the transducers which located above the joints did not detect the cracks formed far from the joints.

3.6 AVERAGE STRAINS PARALLEL TO THE BEAMS

The maximum displacement difference between the slab edges at the bottom of the slab in the direction of the beam was of the order of 1 mm in the slab units no 2 and 6 and 1.5 mm in slab units no 3 and 7. This means that probably there were several cracks in the bottom of the slabs.

The displacement differences between the edges of a slab unit and the corresponding points at the middle beam are presented in Figs 20 and 21. Dividing the displacement difference (cf. Figs 20 and 21) between the measurement points fixed to the structure by the distance between the same points (1060 mm for the top surface and 1120 mm for the bottom surface) the average strain may be obtained.

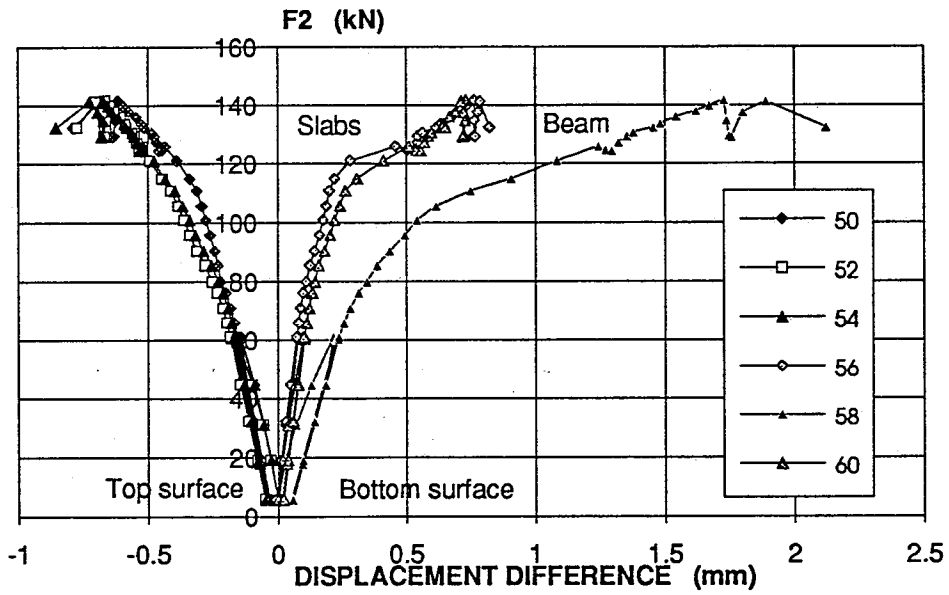

Fig. 20. Displacement differences between the edges of the slab units no 2 and 6 and the corresponding points at the middle beam.

In Fig. 22, the displacement differences in the slab units and in the beam are compared. This figure shows that the reinforced concrete topping makes the top of the floor function monolithically but at the level of the bottom fibre of the slab units, the slab units no 2 and 6 do not perfectly follow the beam.

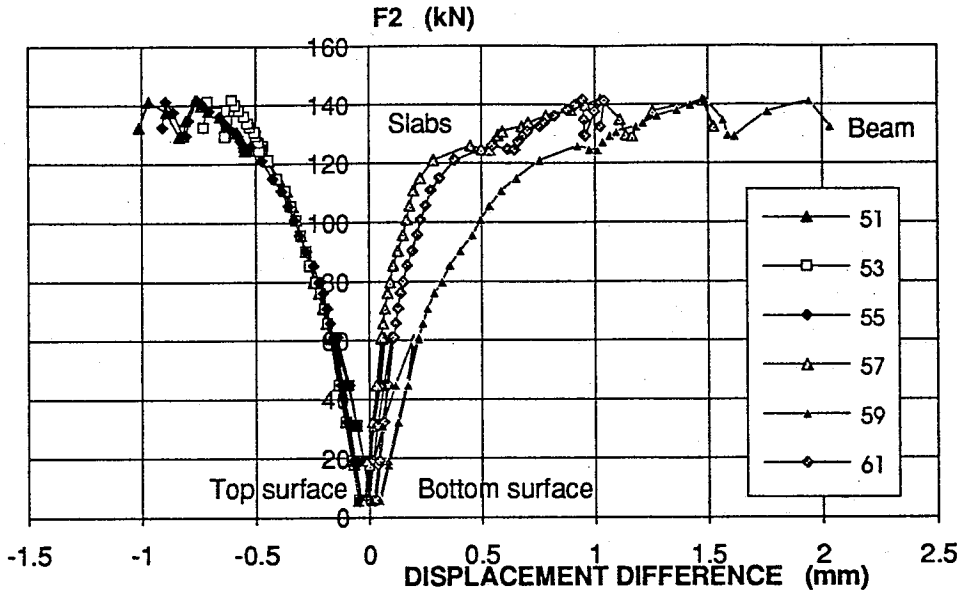

Fig. 21. Displacement differences between the edges of the slab units no 3 and 7 and the corresponding points at the middle beam.

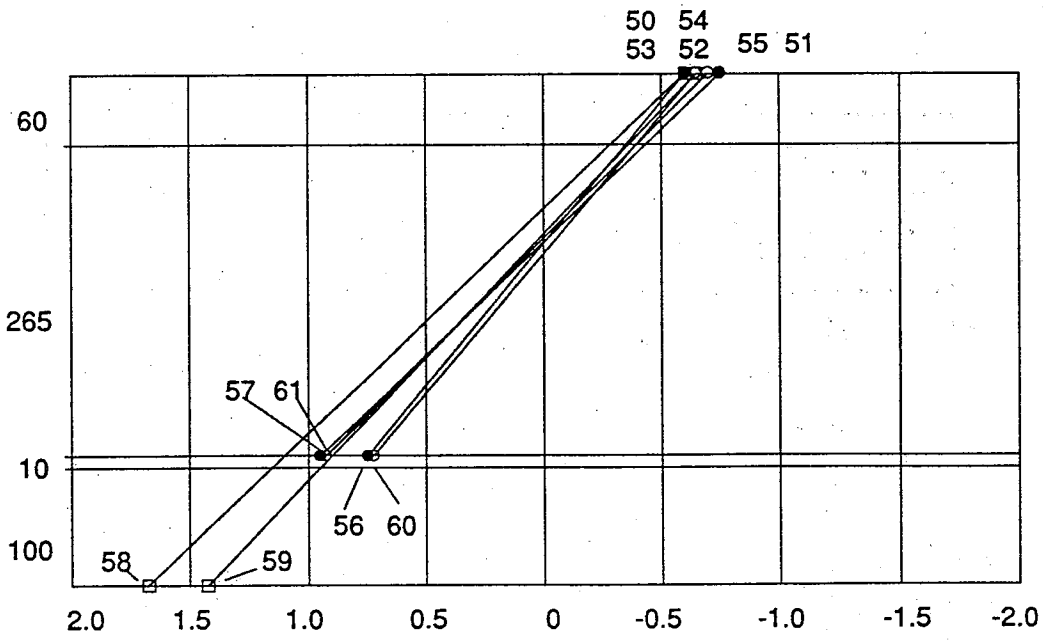

Fig. 22. Displacement differences in the middle beam and hollow core slabs in the direction of the beam when F_2= 139.9 kN (just before the failure). The numbers refer to the transducers. The displacements at the upper surface are connected with a straight line to the corresponding diplacements at the bottom surface.

4 REFERENCE TESTS

4.1 LOADING ARRANGEMENT

On the19th of October, the loading tests on the hollow core units no 9 and 10 were carried out according to the loading arrangement shown in Fig. 23. Both ends of a slab unit were tested. The inductive transducers 1 - 6 measured the deflection, nos 7 and 8 the slip of two outermost strands.

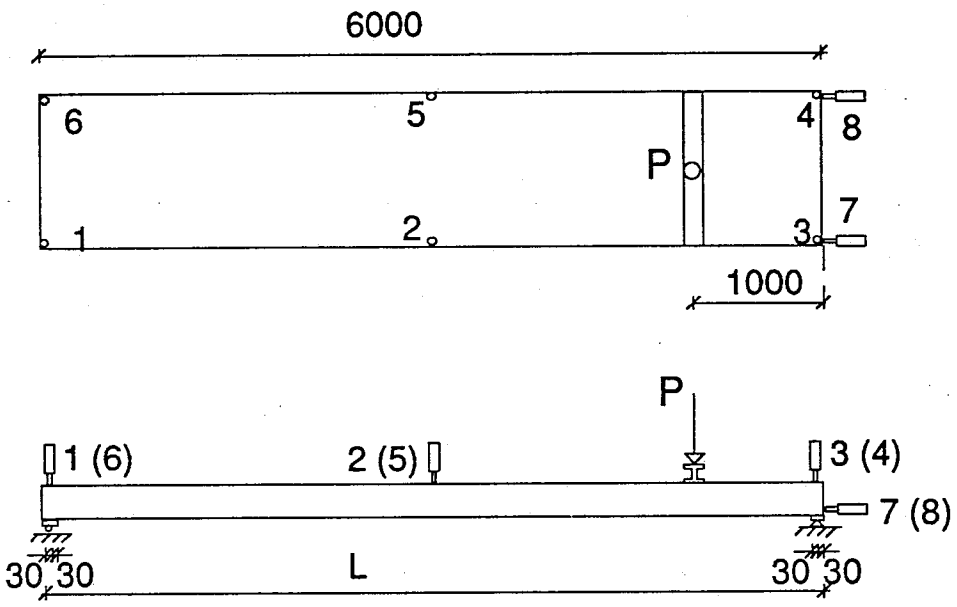

Fig. 23. Layout of a reference test.

4.2 TEST RESULTS

The observed shear capacities and the failure modes of the slab unit no 9 are given in Table 2. The observed weight of the slab unit was equal to 4.2 kN/m, cf. App. 3, and it has been used in the calculation of the ultimate shear force. The test results of the slab unit no 10 have been ignored here because the slab had been manufactured in a different bed than all the other units.

Table 2. Results of the reference tests on the slab units no 9 and 10. L is the span of the unit used in a test, P_u is the ultimate load in a test including the weight of the loading equipment equal to 1.4 kN and V_u is the ultimate shear force including the weight of the slab.

Slab no / test no	L mm	P_u N	V_u kN	Failure mode
9 / 1	5940	233.7	208.0	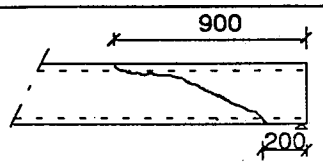
9 / 2	4940	209.3	178.6	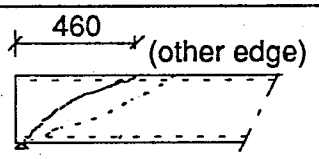

The observed shear capacities of the slab unit 9 were normal. In Figs. 19 - 20 in App. 1 the failure modes of the slabs are also presented.

5 STRENGTH OF CONCRETE

5.1 CONCRETE OF JOINTS, TIE BEAMS AND TOPPING

Two cubes with sizes of 150 mm were cast at the same time as the joints and tie beams, on the 24th of September, and two similar cubes were cast at the same time as the topping, on the 29th of September. The results from the tests on the loading test day, 11th of October, are given in Table 3.

Table 3. Strength and density of 150 mm cubes.

Specimen	Strength MPa	Density kg/m^3
1/ 249	29.5	2180
2/ 249	29.0	2210
3/ 299	29.5	2210
4/ 299	29.0	2190

Three cylinders with a diameter of 50 mm and a height of 50 mm were drilled after the loading test from the joint concrete and six similar cylinders were drilled from the topping concrete. The cylinders were tested on the 25th of October and the results are presented in Tables 4 and 5.

Table 4. Strength and density of joint concrete from 50 mm cylinder tests.

Specimen	Strength MPa	Density kg/m^3
S1	32.0	2140
S2	36.5	2160
S3	33.0	2140
Mean value	33.8	2147

Table 5. Strength and density of the topping concrete from 50 mm cylinder tests.

Specimen	Strength MPa	Density kg/m^3
P1	33.5	2220
P2	32.0	2200
P3	35.5	2180
P4	35.0	2210
P5	34.5	2190
P6	34.5	2200
Mean x	34.2	2200
Standard deviation s	1.25	14
Characteristic strength $f_{ck,\ C50} = x\text{-}1.65s$	32.1	

5.2 SLAB UNITS

After the loading and the reference tests, eighteen cylinders with a diameter of 50 mm and a height of 50 mm were drilled from the slab units. Six cylinders were drilled from the tested floor and six from the slab unit no 9. They were tested on 25th of October. The results are given in Tables 6 and 7.

Table 6. Strength and density of 50 mm cylinders drilled from the floor slab units nos 1, 3 and 8.

Specimen	Strength MPa	Density kg/m^3
1a	83.0	2440
1b	81.5	2410
3a	71.0	2390
3b	77.5	2440
8a	79.5	2410
8b	76.5	2410
Mean x	78.2	2417
Standard deviation s	4.3	20
Characteristic strength $f_{ck,C50} = x - 1.65s$	71.1	

Table 7. Strength and density of 50 mm cylinders drilled from the slab unit no 9.

Specimen	Strength MPa	Density kg/m^3
91	77.5	2430
92	71.5	2430
93	63.0	2390
94	73.5	2380
95	74.0	2410
96	72.5	2400
Mean x	72.0	2407
Standard deviation s	4.9	21
Characteristic strength $f_{ck,\ C50} = x - 1.65s$	64.0	

5.3 THE MIDDLE BEAM

In Table 8 the strength and density of six cylinders 75 in diameter and 75 mm in height drilled from the concrete middle beam and tested on the 25th of October are given.

Table 8. Strength and density of the middle beam concrete from 75 mm cylinders.

Specimen	Strength MPa	Density kg/m^3
KP1	66.0	2380
KP2	66.5	
KP3	64.0	2390 2400
KP4	56.5	2370
KP5	62.0	2390
KP6	62.5	2390
Mean value x	62.9	2387
Standard deviation s	3.6	10
Characteristic strength $f_{ck,\ C75} = x - 1.65s$	56.9	

6 COMPARISON OF THE FLOOR TEST RESULT TO THE RESULTS OF THE REFERENCE TESTS

The observed shear capacity of the hollow core slab units in the floor test was equal to 140.2 kN. The mean value of the shear capacities obtained from reference test results was 193.3 kN. This means that the shear capacity of a hollow core slab supported on a concrete beam and having a concrete topping of 60 mm in depth was 72.5 % of that observed from a loading test on a slab supported on the wall-like, non-flexible supports.

7 DISCUSSION OF THE RESULTS

1. No problems arose when assembling the floor specimen. The concreting of the joints, edge beams and topping succeeded perfectly. In addition to the cleaning and wetting of the top surface of the hollow core units and the middle beam, there was no special treatment before the topping concrete was cast. The strength of the concrete in all structural components as well as the shear capacity of the hollow core unit no 9 measured in the reference test were typical of the ordinary production. For these reasons the specimen may be regarded as representative.

2. The end beams underwent approximately the same deflection as the middle beam until 90% of the failure load.

3. Visible cracks parallel to the beam were observed in the topping at the middle beam at a relatively late stage. The crack widths (sum of crack widths) were also small, less than 1 mm at failure. This may be explained by the location of the line loads close to the middle beam and by the structural topping which reduced the deflection of the hollow core slabs and hence also the crack widths at the supporting beam.

4. Due to the topping, the deflections of the floor were considerably smaller than those in a former test without topping under the same load (cf. [1], floor test PC265).

5. The outermost hollow core units underwent a web shear failure when the support reaction of the hollow core units was equal to 140.2 kN. In the corresponding floor test PC265 without topping the support reaction at failure was equal to 103.8 kN. In the floor test PC265E without topping (cf. [1]) where the voids were filled with concrete (filling length equal to 185 mm) and where the loading was more evenly distributed, the support reaction at failure was equal to 146.8 kN. Although there were some differences in the material parameters in the various tests, it may be concluded that the effect of the present topping on the shear capacity of the hollow core units was of the same order as that of the concrete infill in the voids in the test PC265E.

6. As can be seen from the load-deflection curves of the middle beam, the floor showed considerable ductility at failure. The hollow core units failed when the yielding of the middle beam had started. The obtained shear capacity was maximum in the sense that the hollow core units cannot resist the torsional stresses due to the yielding of one of the supporting beams.

7. Using the calculation method presented in the *Design Recommendations* [2] and the material parameters obtained from the test specimen, the observed failure load is obtained if the calculated horizontal shear stress in the direction of the beam is multiplied by a factor of 0.67.

8. The obtained shear capacity was higher than in the case without topping because the reinforced concrete topping reduced the shear deformation of the hollow core slabs in the direction of the beam. This reduction depends on the width of the vertical crack in the joint concrete and topping along the beam.: the wider the crack, the greater the shear deformation and the lower the shear capacity. In the present floor test the line loads were close to the middle beam. If the floor were subjected to an evenly distributed load, the crack widths would have been much wider and the observed shear capacity presumably lower. Therefore, some conservatism is necessary when applying the obtained result.

REFERENCES

[1] Pajari, M. and Yang, Lin. Shear capacity of hollow core slabs on flexible supports. VTT, Laboratory of Structural Engineering. Internal Report RAT-IR-6/1993. Espoo 1993.

[2] Pajari, M. (ed). Design Recommendations for hollow core slabs on flexible supports. VTT, Laboratory of Structural Engineering. Internal Report RAT-IR-2/1993. Espoo 1993.

APPENDICES

PHOTOGRAPHS ON THE LOADING TEST

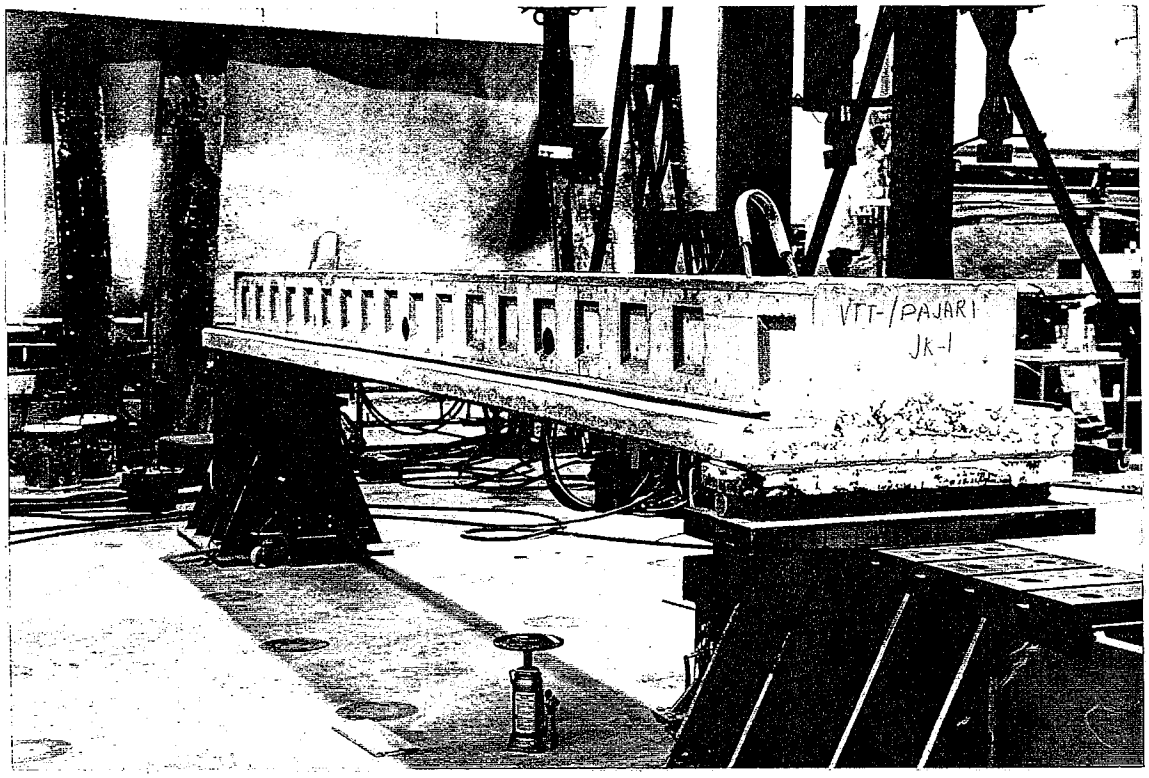

Fig 1. The prestressed concrete middle beam on the supports.

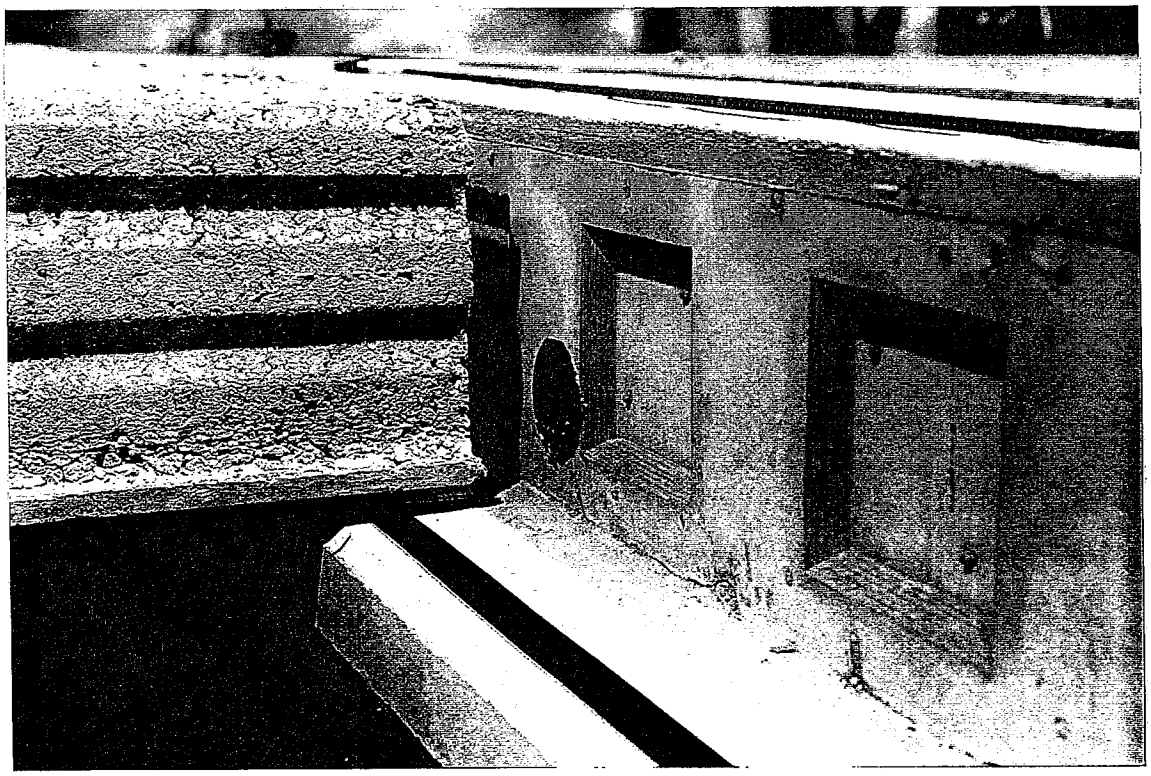

Fig. 2. A hollow core slab unit supported on the middle beam.

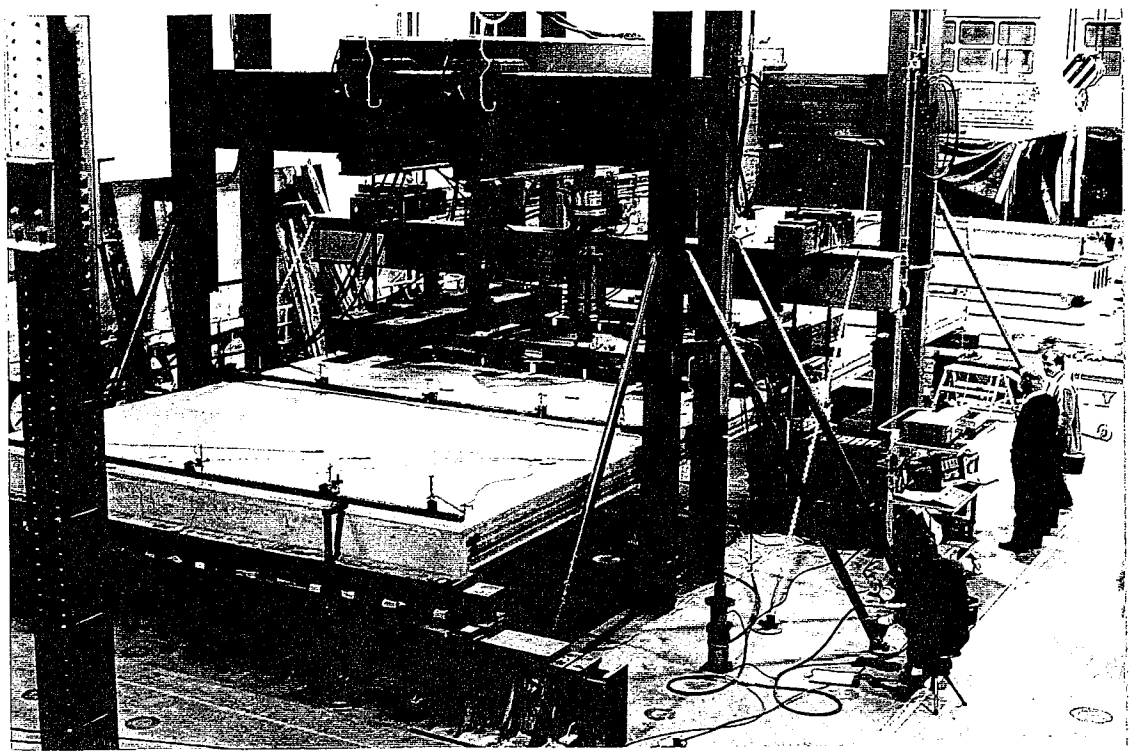

Fig. 3. Loading and measurement arrangement.

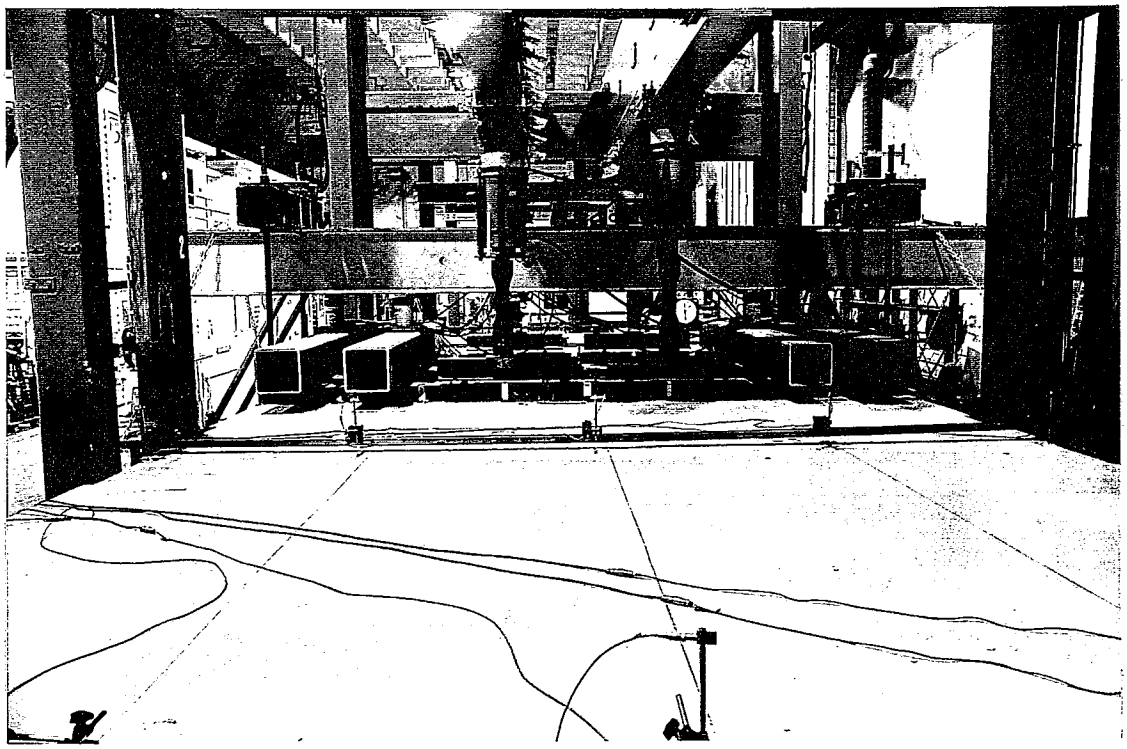

Fig. 4. Loading arrangement.

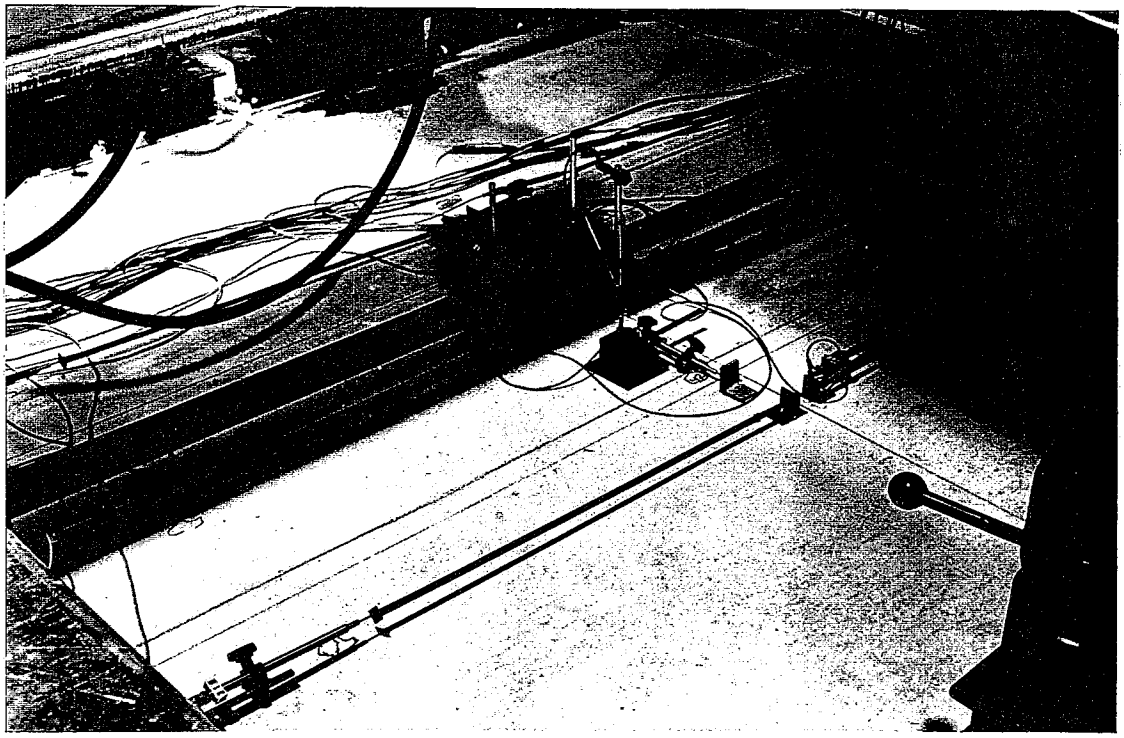

Fig. 5. Measurements for the displacement difference between the middle beam and the end of a slab unit and that one between the edges of a slab unit on the surface of the concrete topping.

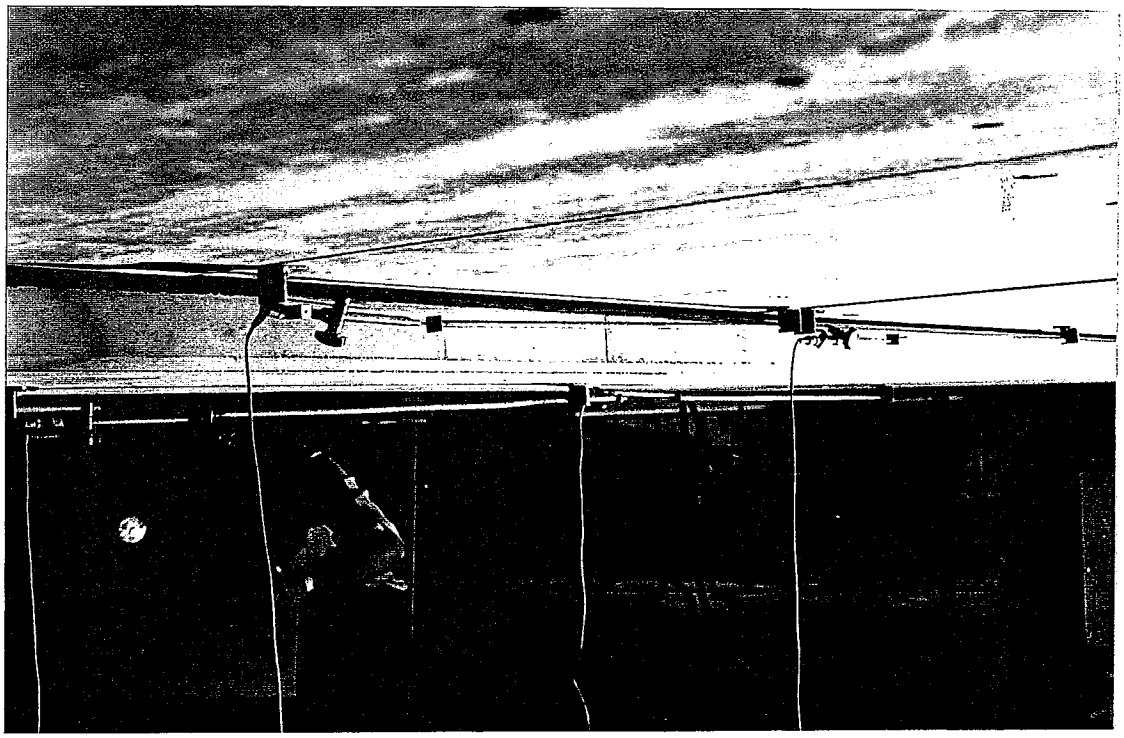

Fig. 6. Measurement for the displacement difference between the edges of a slab unit on the bottom of the slab.

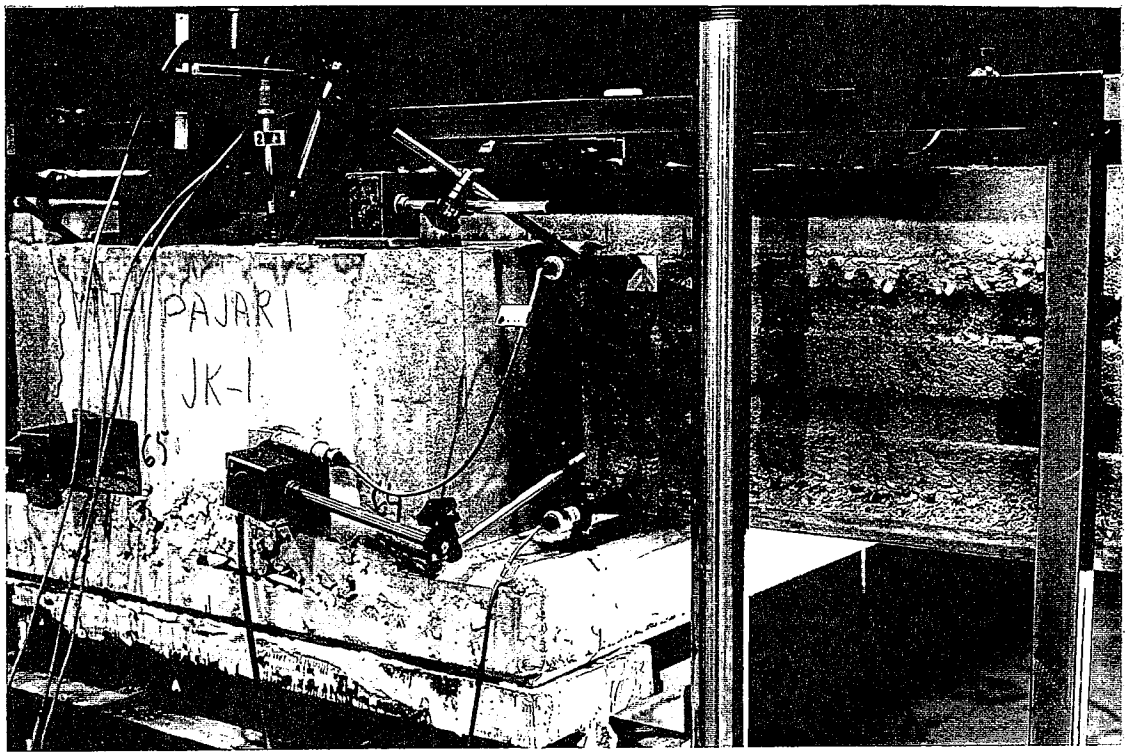

Fig. 7. Measurement for the displacement difference between the end of the middle beam and the edge of a slab unit.

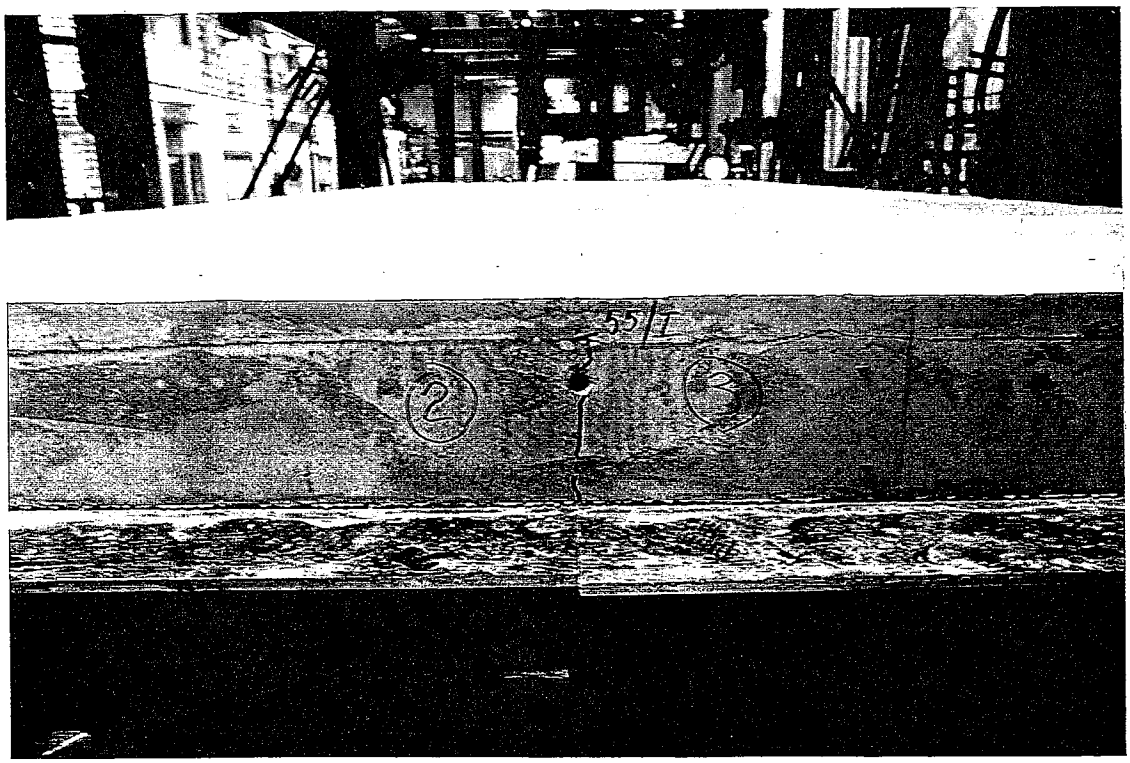

Fig. 8. A crack in the middle of the concrete tie beam, between the slab unit no 2 and 3.

Fig. 9. A crack in the middle of the concrete tie beam, between the slab units no 6 and 7.

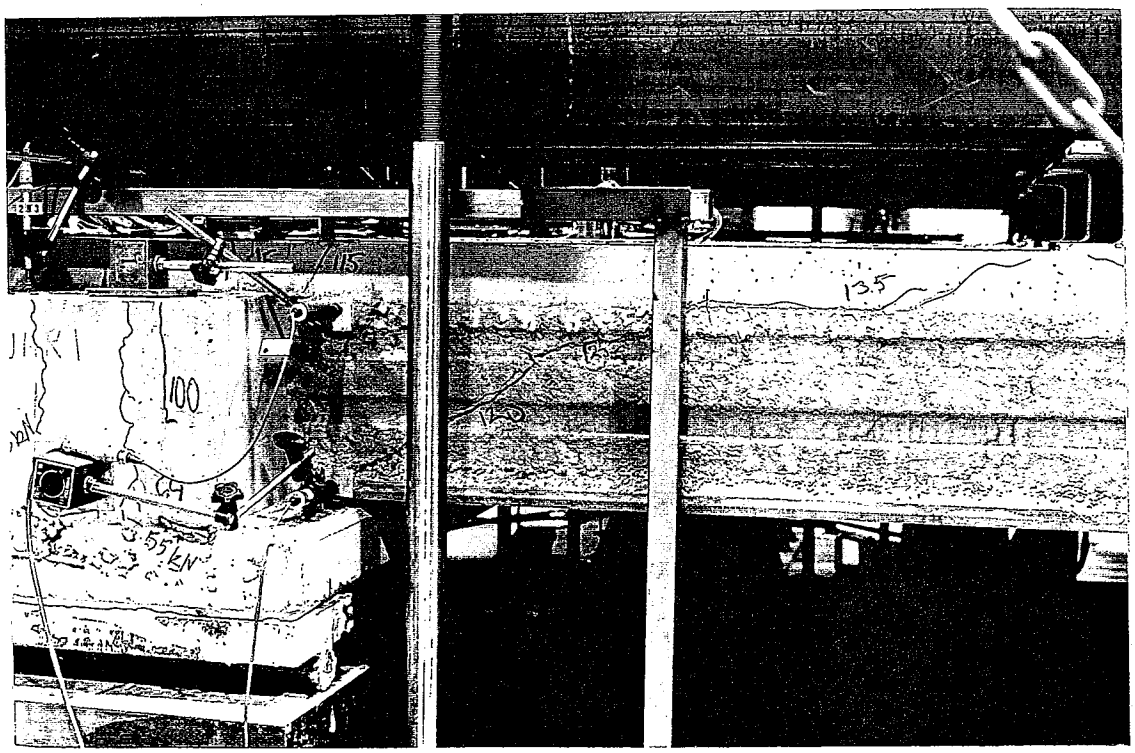

Fig. 10. The cracks in the longitudinal edge of the slab unit no 1, near the middle beam, at failure.

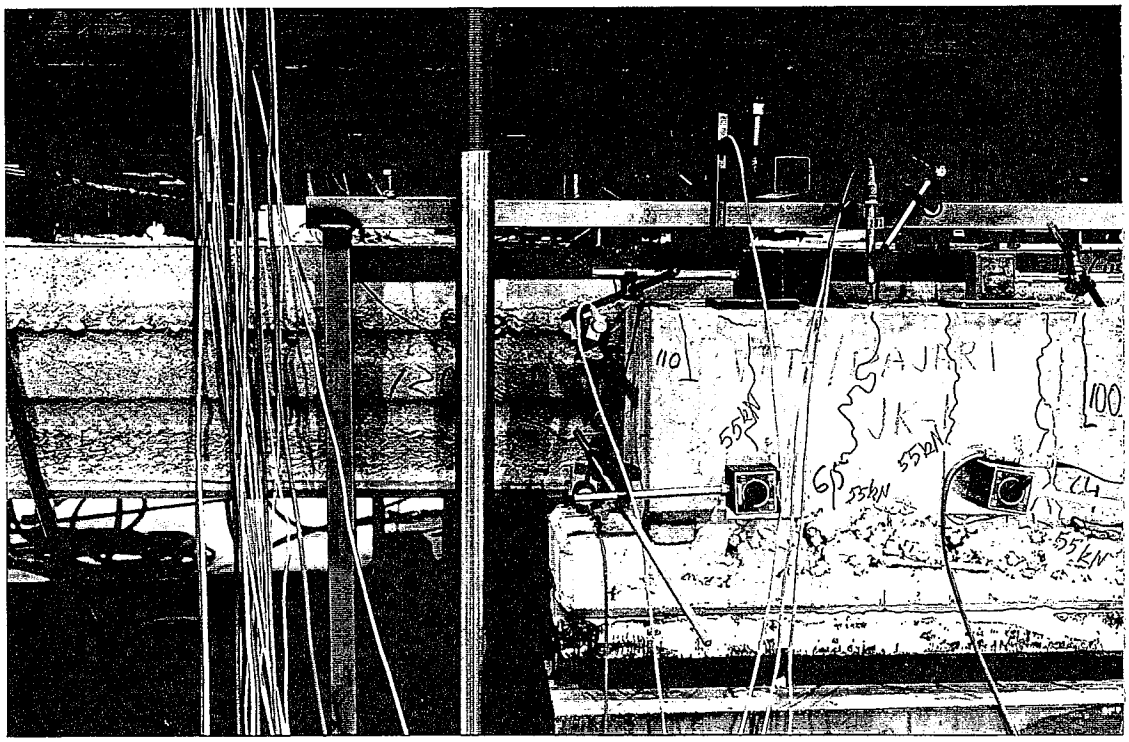

Fig. 11. The cracks in the longitudinal edge of the slab unit no 5, near the middle beam, at failure.

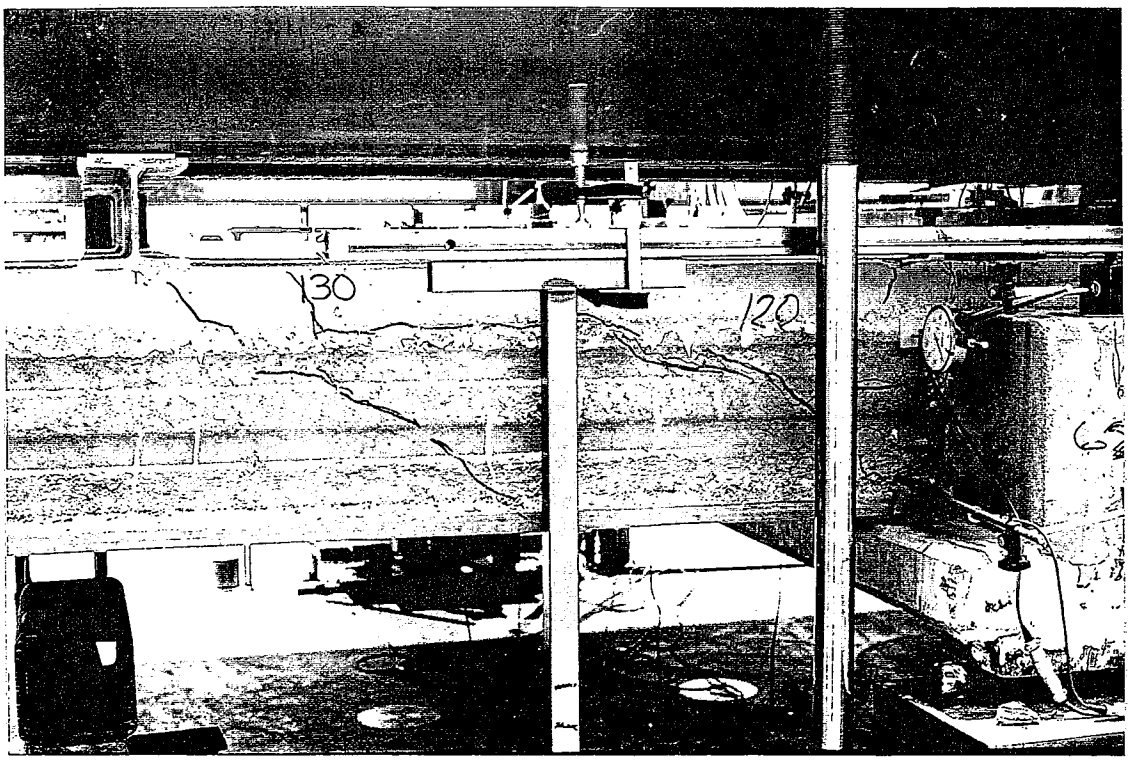

Fig. 12. The cracks in the longitudinal edge of the slab unit no 4, near the middle beam, at failure.

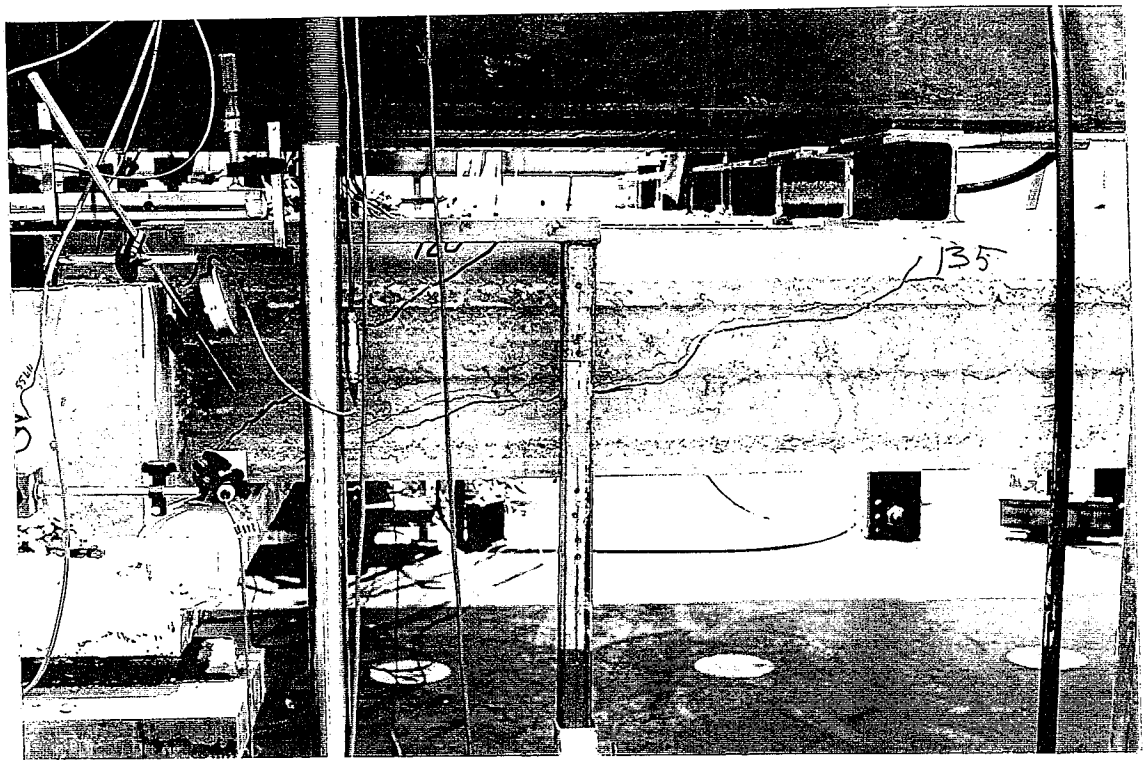

Fig. 13. The cracks in the longitudinal edge of the slab unit no 8, near the middle beam, at failure.

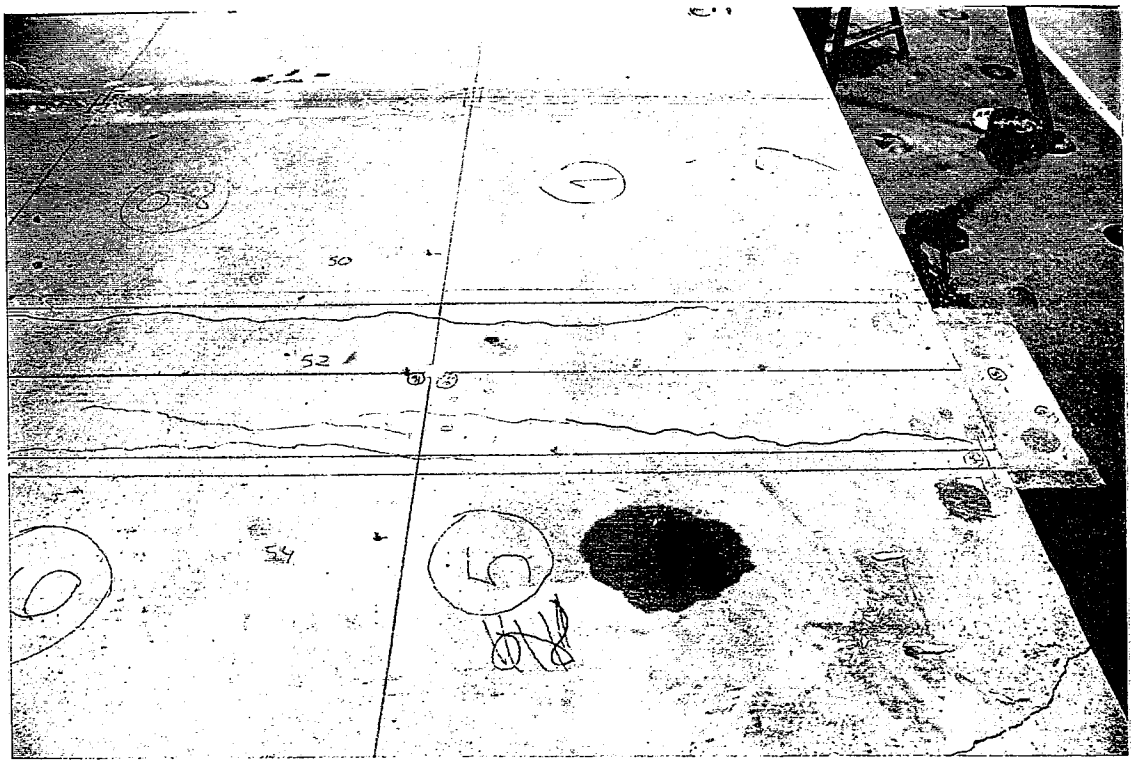

Fig. 14. The cracking of the concrete topping along the joint between the middle beam and the ends of the slab units no 1 - 2 and no 5 - 6.

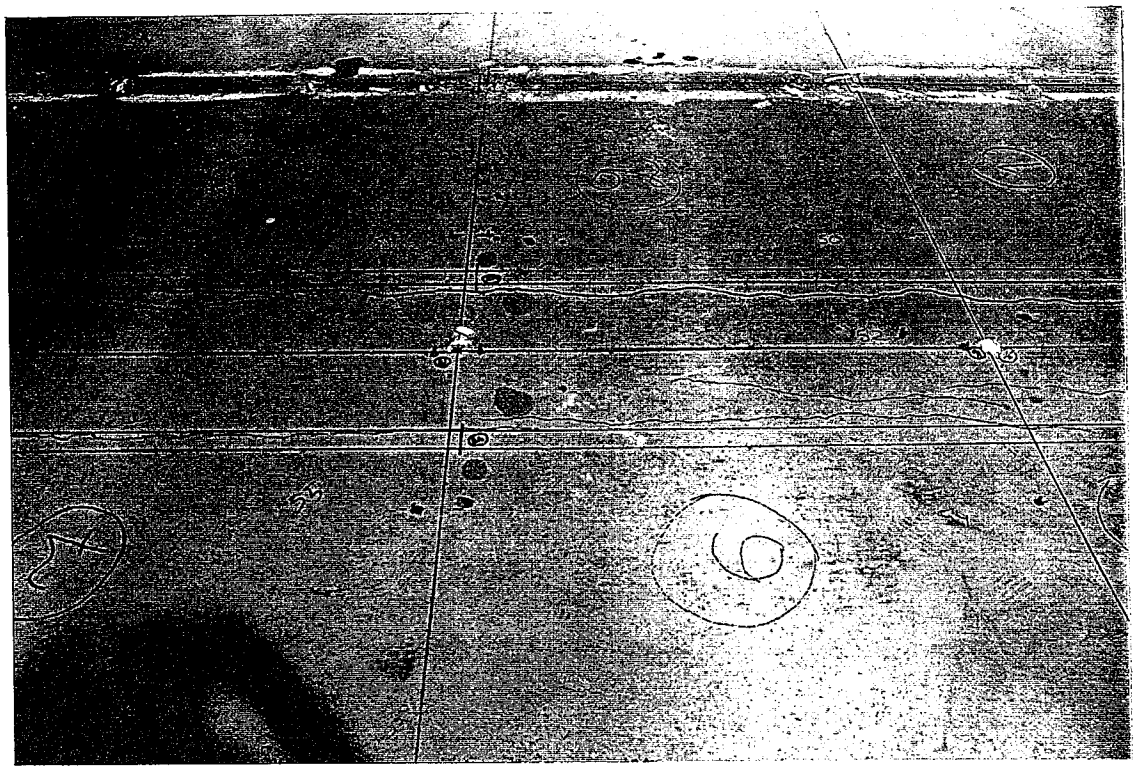

Fig. 15. The cracking of the concrete topping along the joint between the middle beam and the ends of the slab units no 1 - 3 and no 6 - 7.

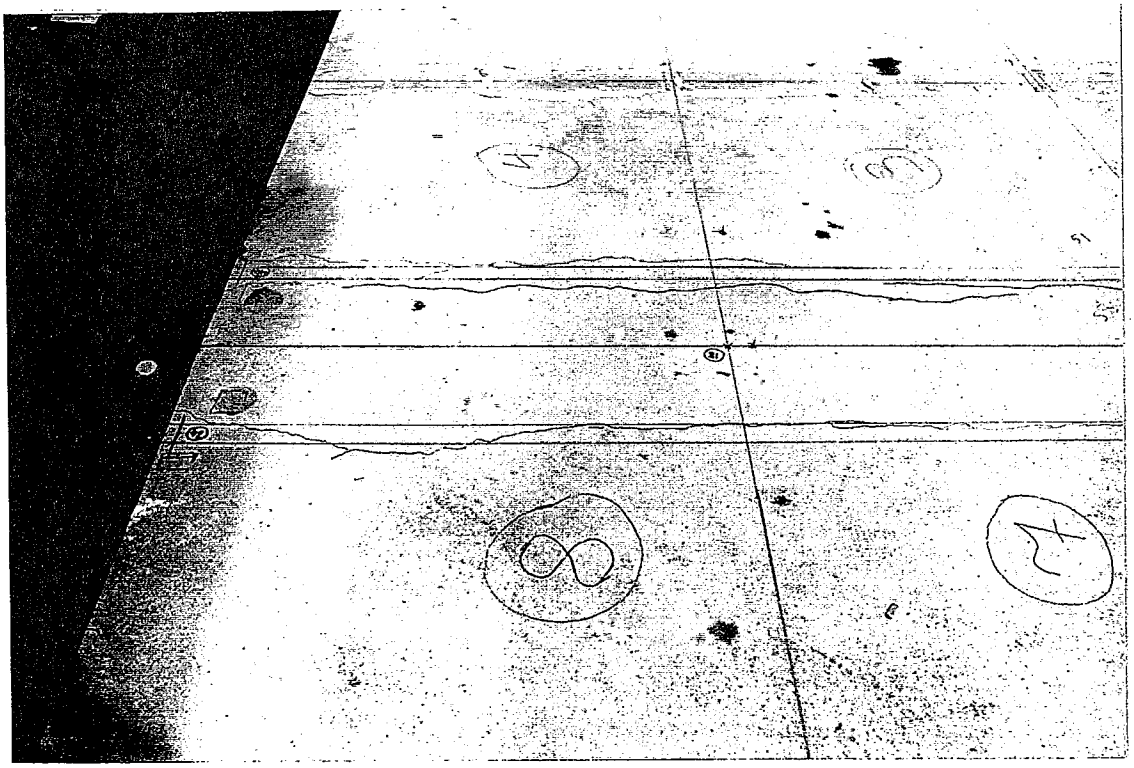

Fig. 16. The cracking of the concrete topping along the joint between the middle beam and the ends of the slab units no 3 - 4 and no 7 - 8.

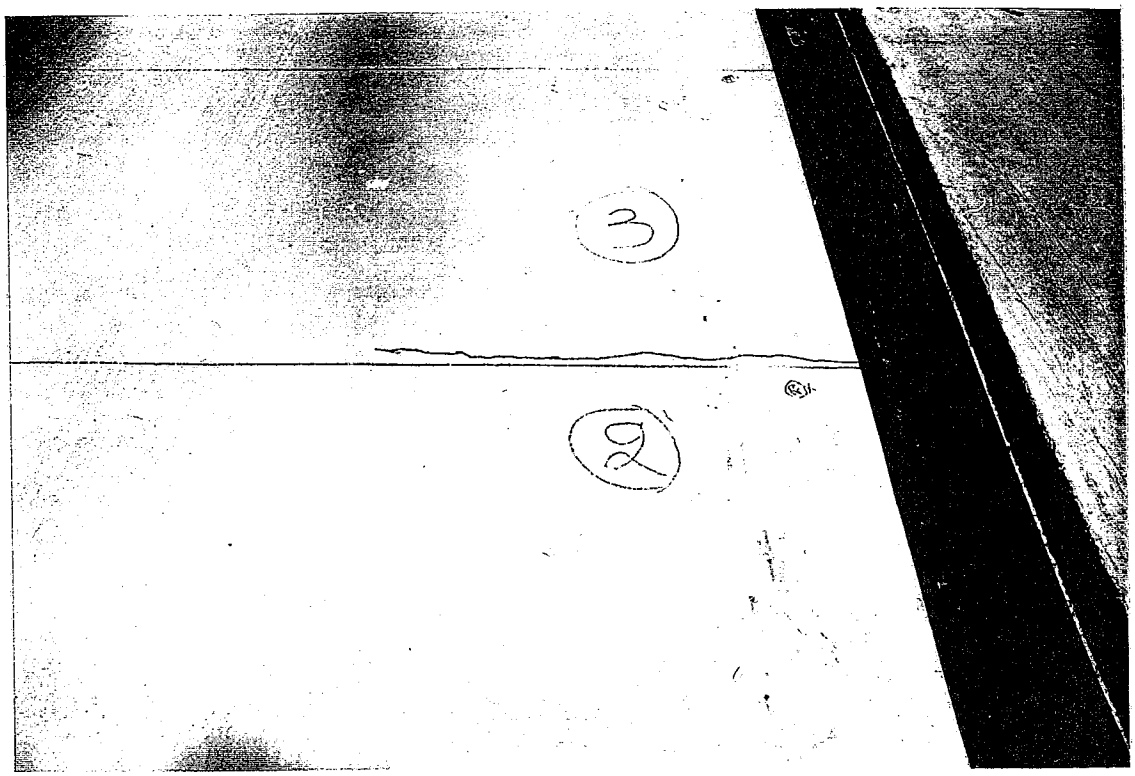

Fig. 17. The cracking of the concrete topping and the tie beam between the slab units no 2 and 3.

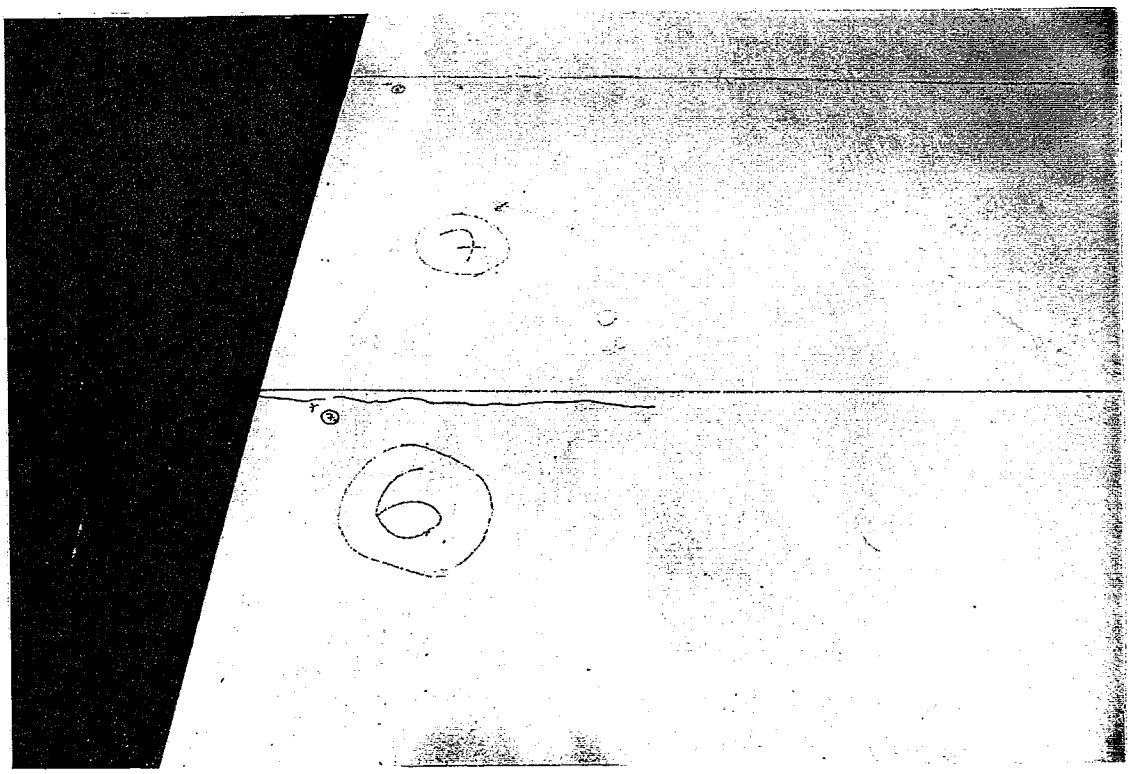

Fig. 18. The cracking of the concrete topping and the tie beam between the slab units no 6 and 7.

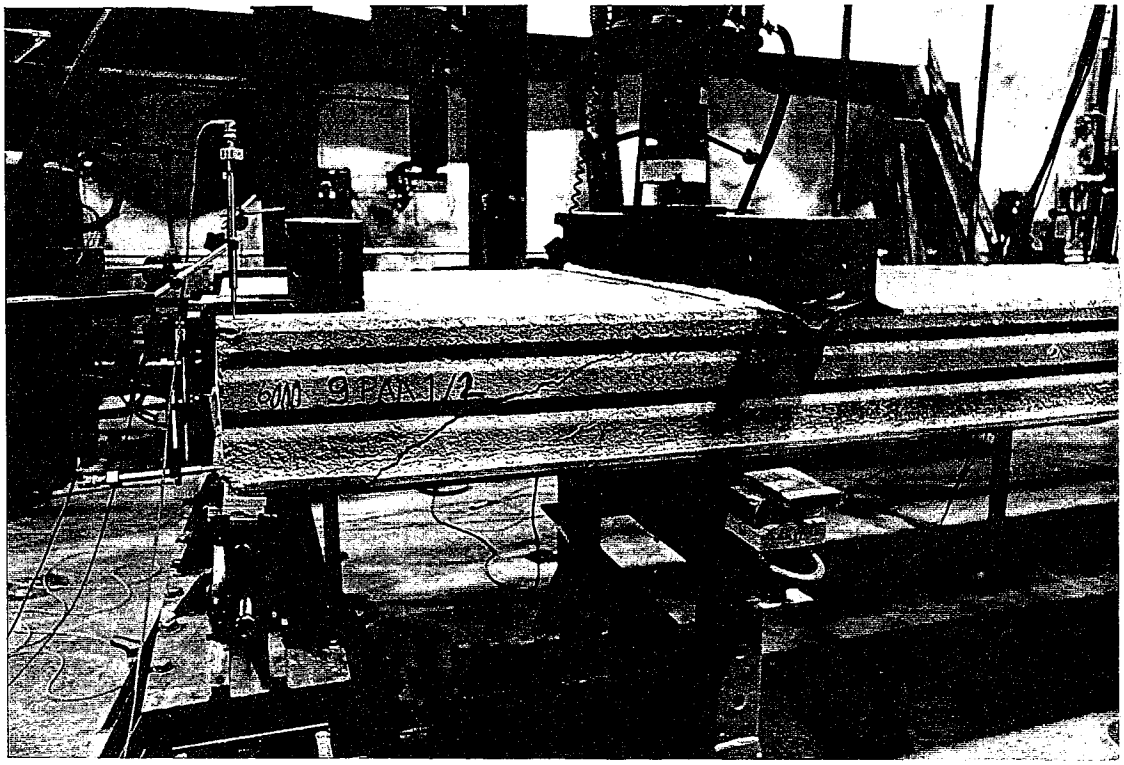

Fig. 19. The failure of the end 1 of the slab unit no 9 in the reference loading test.

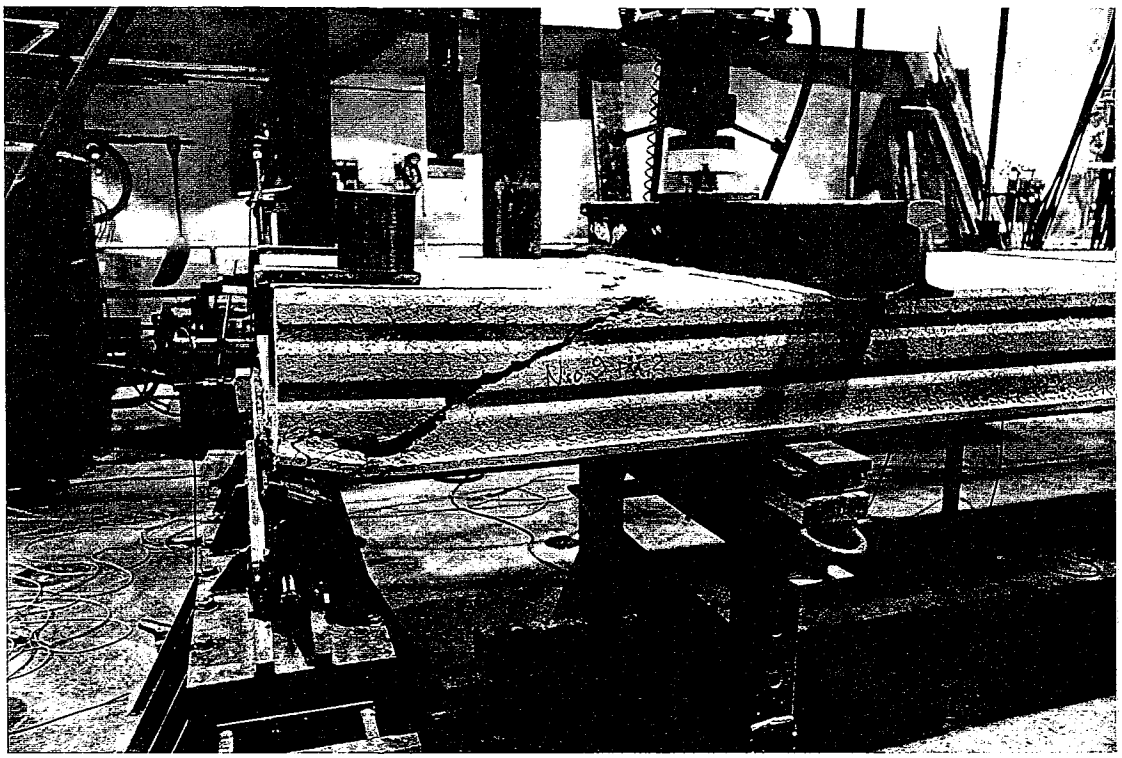

Fig. 20. The failure of the end 2 of the slab unit no 9 in the reference loading test.

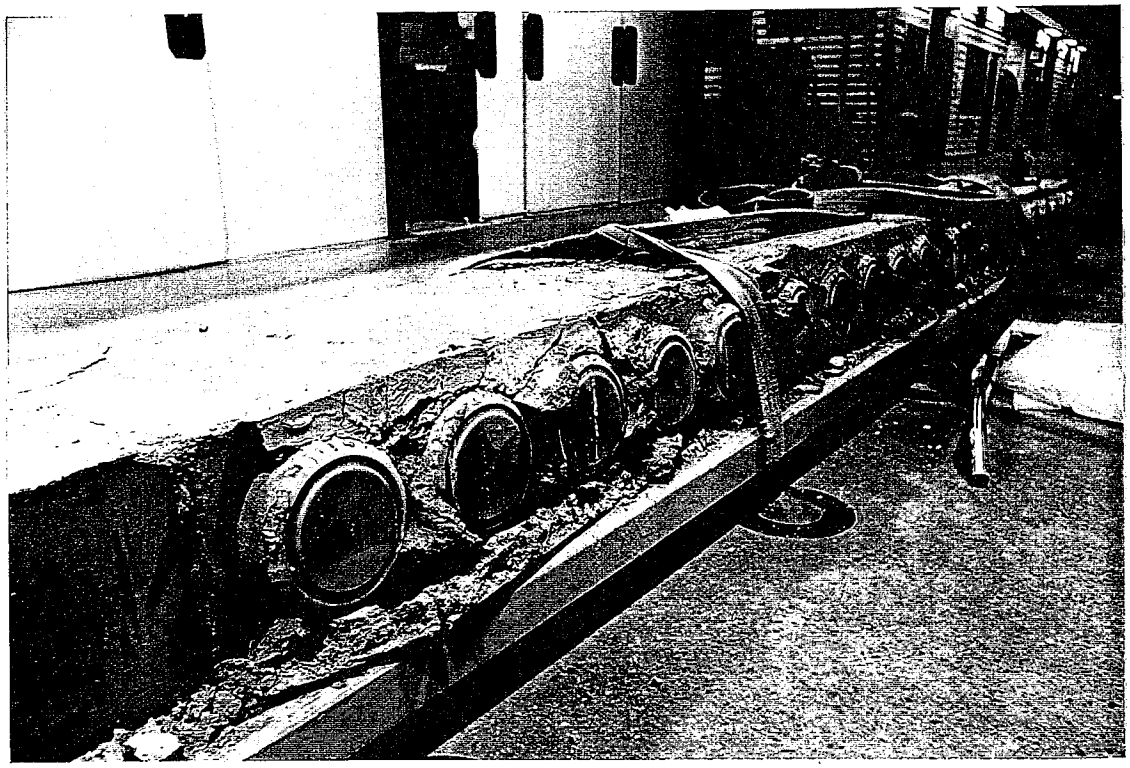

Fig. 21. The middle beam after the loading test, on the side of the slab units no 1 - 4.

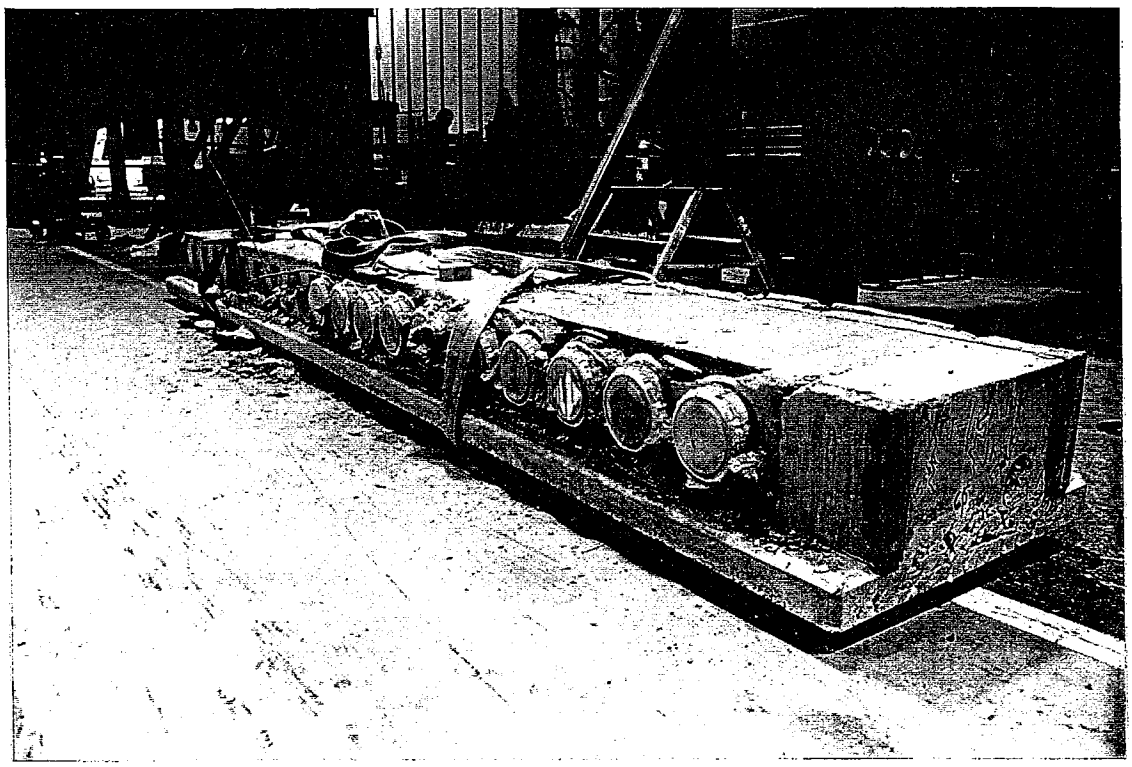

Fig. 22. The middle beam after the loading test, or the side of the slab units no 5 - 8.

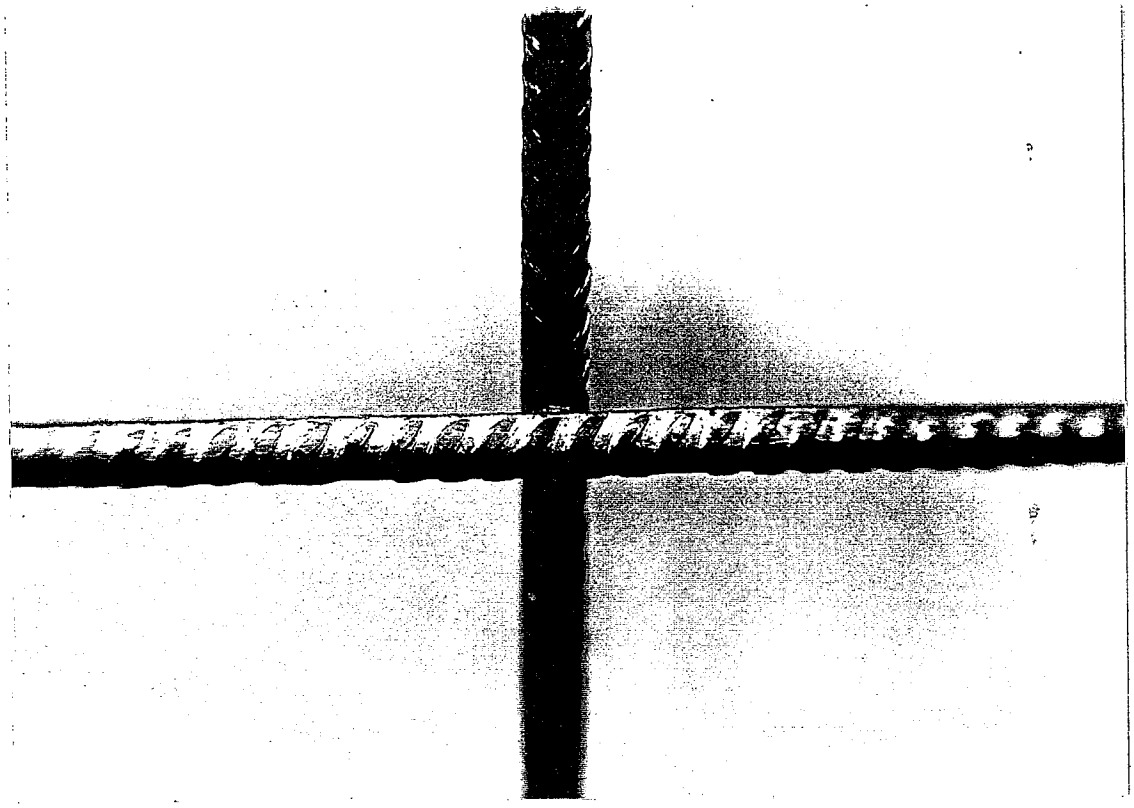

Fig. 23. The surface deformations of a bar in a mesh reinforcement.

MAIN CHARACTERISTICS OF THE BEAMS AND THE MESH REINFORCEMENT

In the middle beam the prestressing steel was of the type St 1570/1770. The concrete grade was K60 and the cubic strength of concrete when transferring the prestressing force was K40.

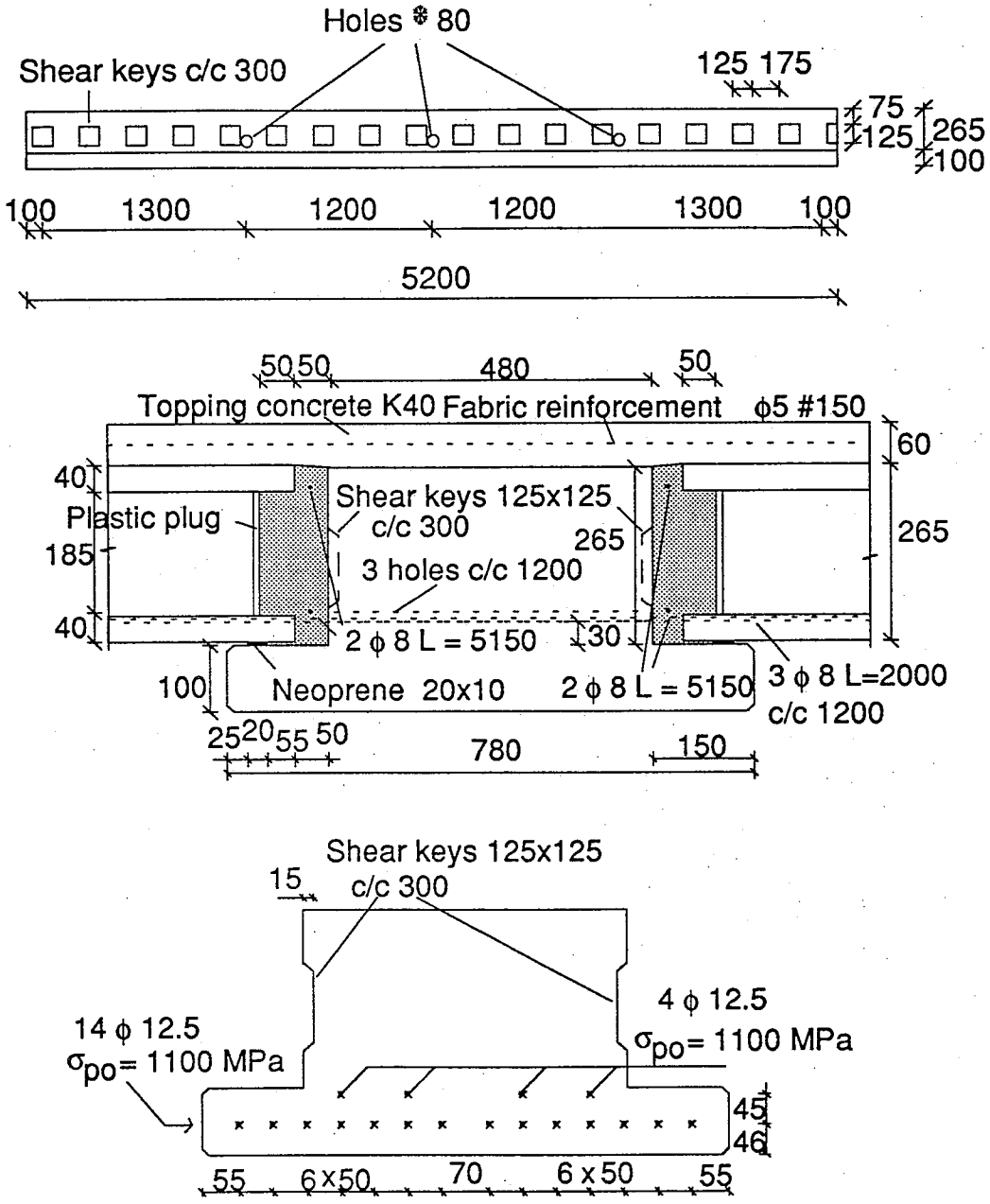

Fig. 1. Middle beam.

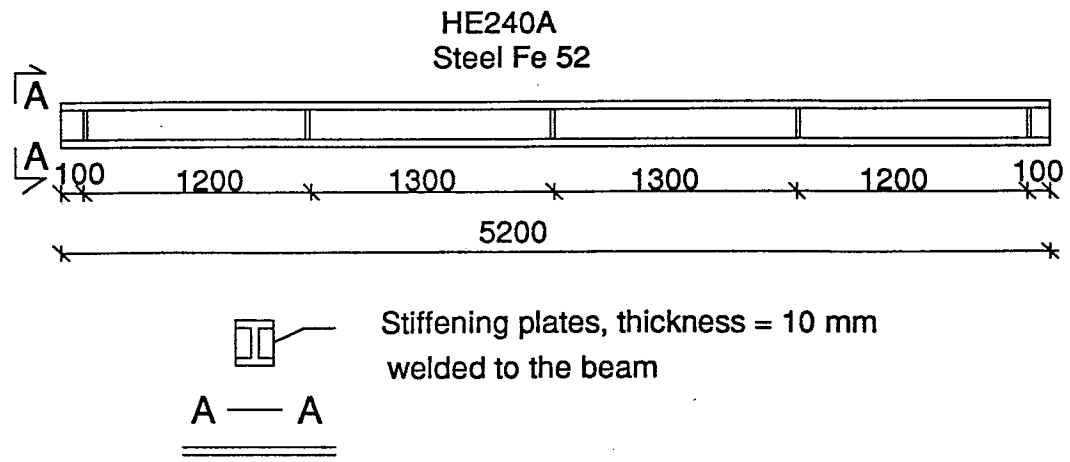

Fig. 2. End beams.

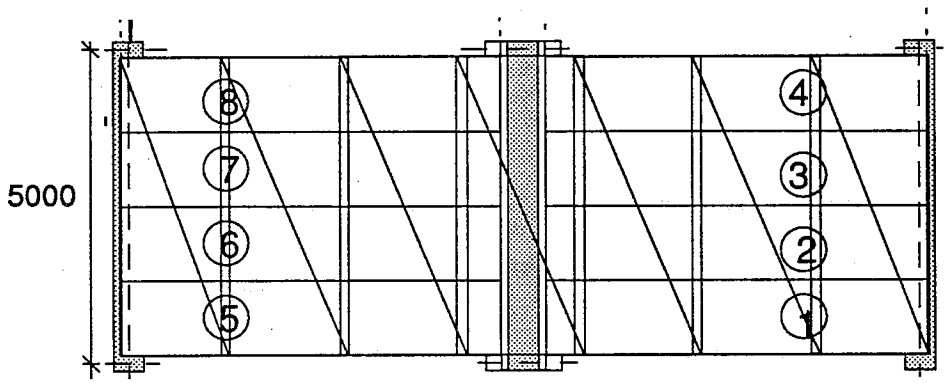

Fig. 3.. Placement of the mesh reinforcement over the floor.

APPENDIX 3

GEOMETRY OF SLAB NO 1

STRAND: 10 ø 12,5
STRESS: 950 N/mm^2

LENGTH: 6005 MM
WEIGHT: 2550 kg

END 1 / EDGE 1 — END 1 / EDGE 2

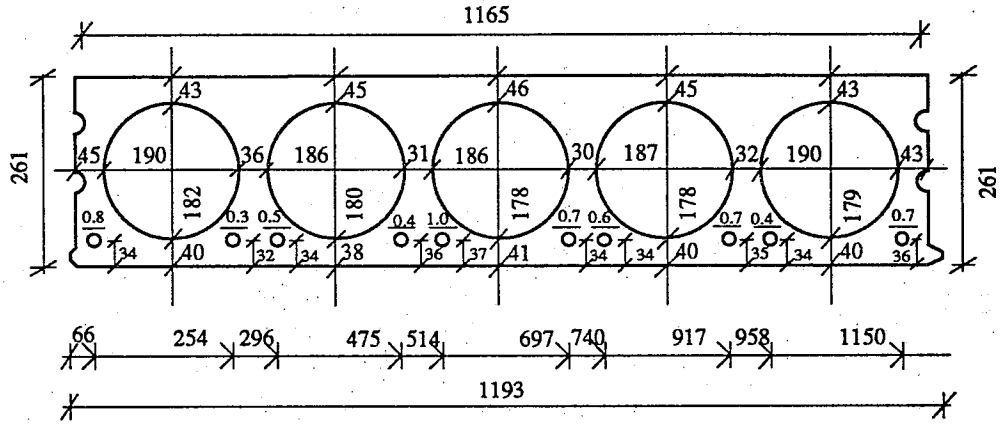

END 2 / EDGE 1 — END 2 / EDGE 2

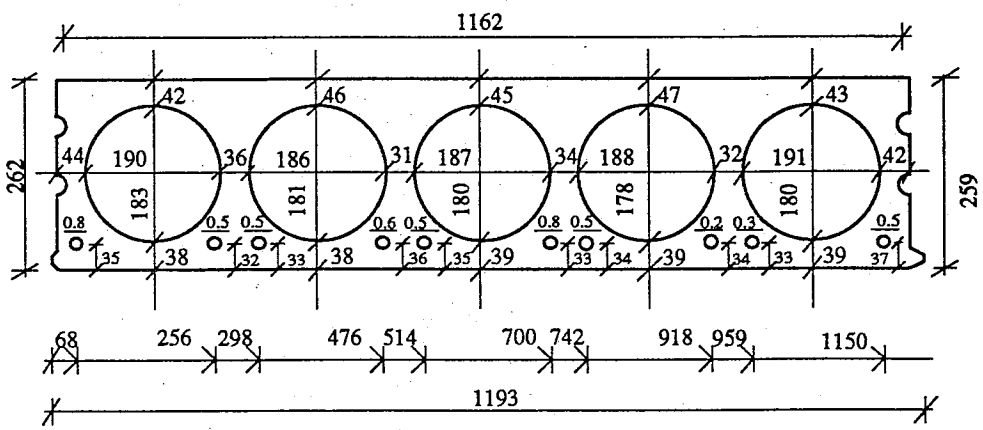

GEOMETRY OF SLAB NO 2

STRAND: 10 ø 12,5
STRESS: 950 N/mm^2

LENGTH: 5992 mm
WEIGTH: 2560 kg

END 1 / EDGE 1

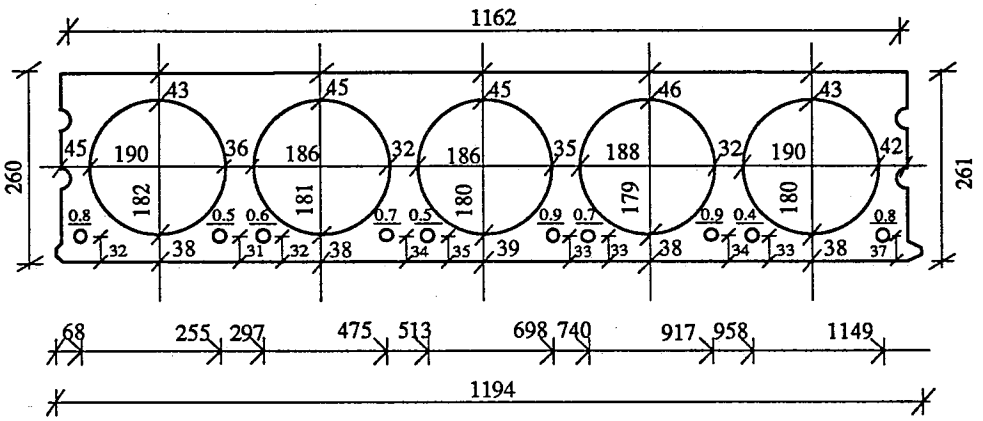

END 1 / EDGE 2

END 2 / EDGE 1

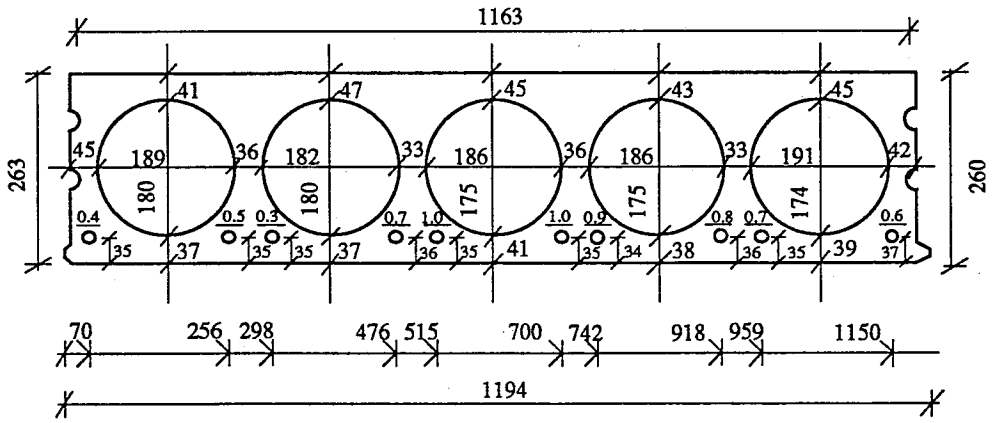

END 2 / EDGE 2

GEOMETRY OF SLAB NO 3

STRAND: 10 ø 12,5
STRESS: 950 N/mm^2

LENGTH: 6000 mm
WEIGHT: 2540 kg

END 1 / EDGE 1

END 1 / EDGE 2

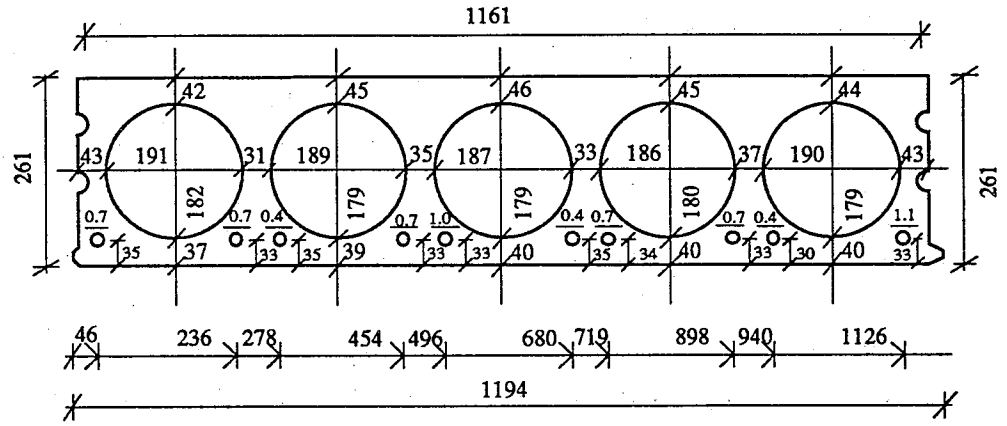

END 2 / EDGE 1

END 2 / EDGE 2

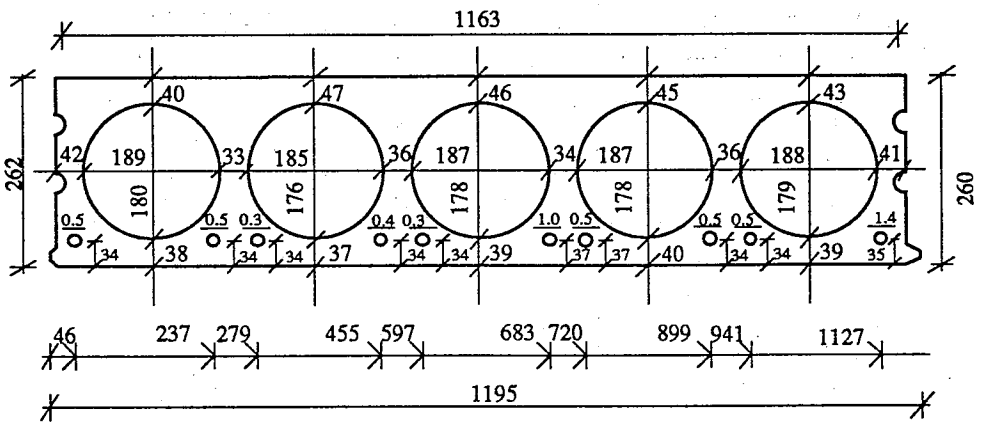

GEOMETRY OF SLAB NO 4

STRAND: 10 ø 12,5
STRESS: 950 N/mm^2

LENGTH: 5999 mm
WEIGHT: 2550 kg

END 1 / EDGE 1 END 1 / EDGE 2

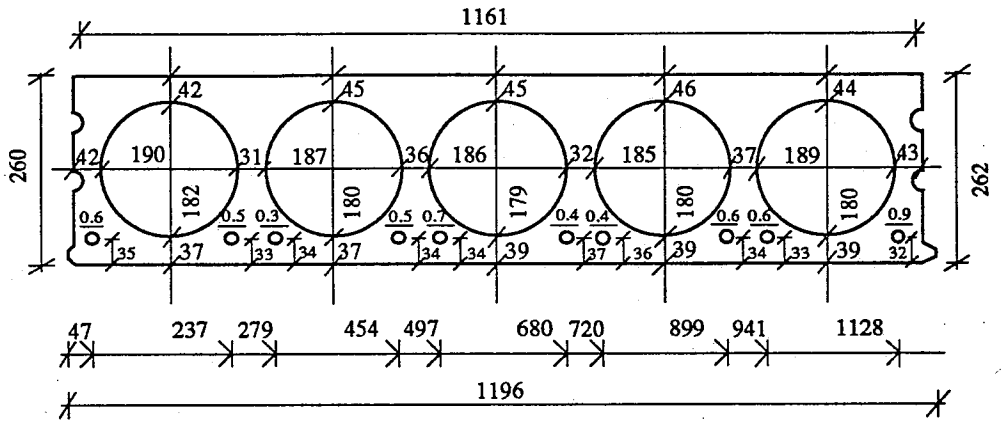

END 2 / EDGE 1 END 2 / EDGE 2

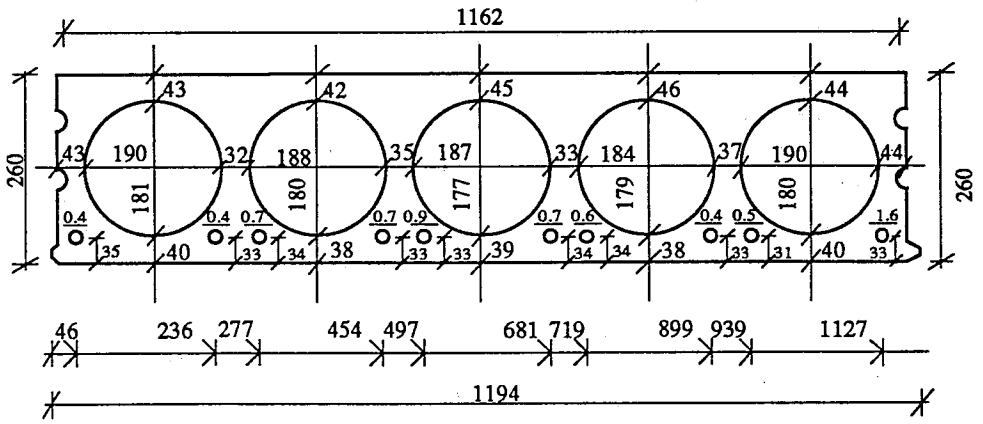

APPENDIX 3

5/10

GEOMETRY OF SLAB NO 5

STRAND: 10 ø 12,5
STRESS: 950 N/mm^2

LENGTH: 6004 mm
WEIGHT: 2560 kg

END 1 / EDGE 1 — END 1 / EDGE 2

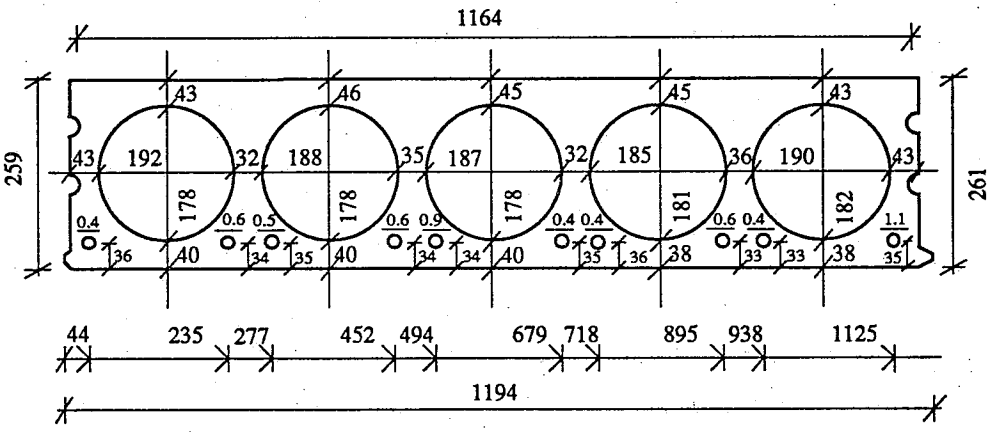

END 2 / EDGE 1 — END 2 / EDGE 2

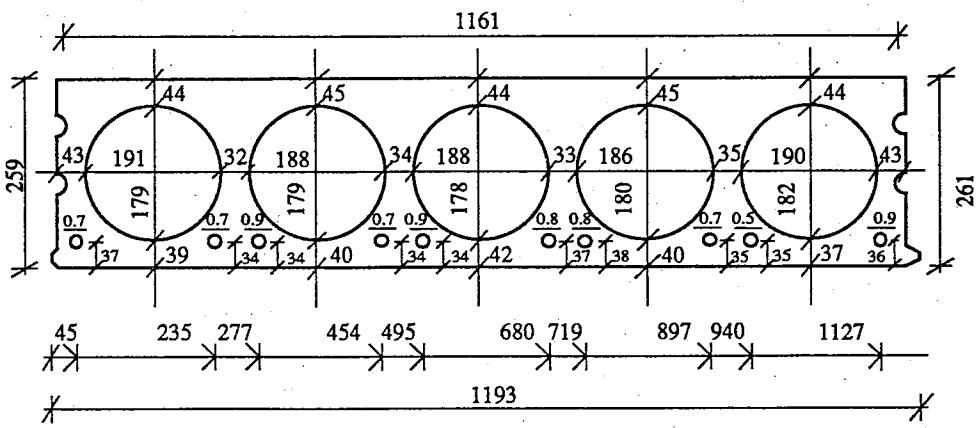

GEOMETRY OF SLAB NO 6

STRAND: 10 ø 12,5
STRESS: 950 N/mm2

LENGTH: 6004 mm
WEIGHT: 2560 kg

END 1 / EDGE 1

END 1 / EDGE 2

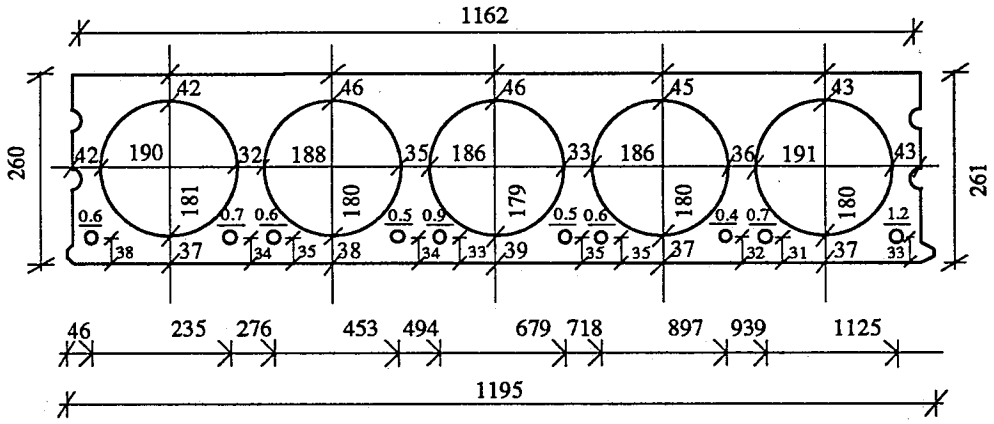

END 2 / EDGE 1

END 2 / EDGE 2

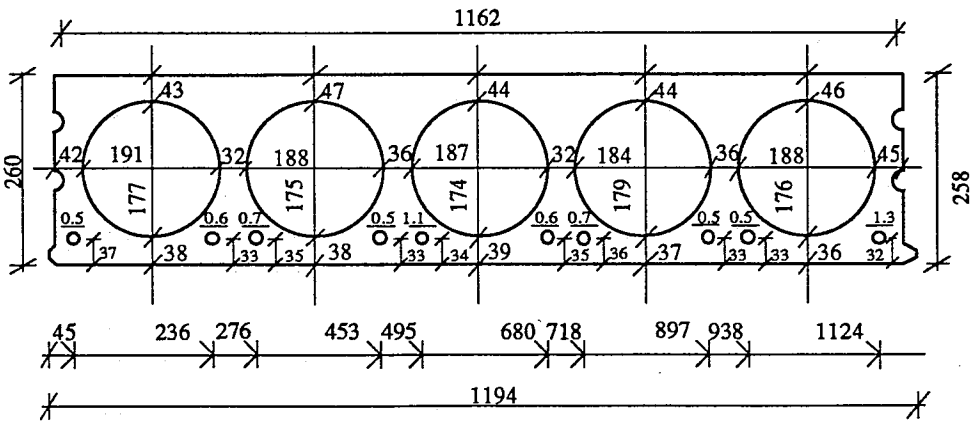

GEOMETRY OF SLAB NO 7

STRAND: 10 ø 12.5
STRESS: 950 N/mm^2

LENGTH: 5997 mm
WEIGHT: 2560 kg

END 1 / EDGE 1

END 1 / EDGE 2

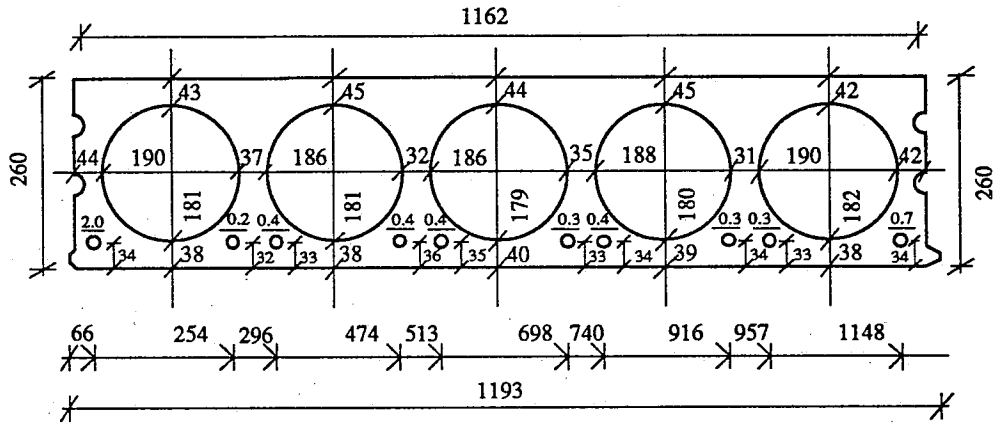

END 2 / EDGE 1

END 2 / EDGE 2

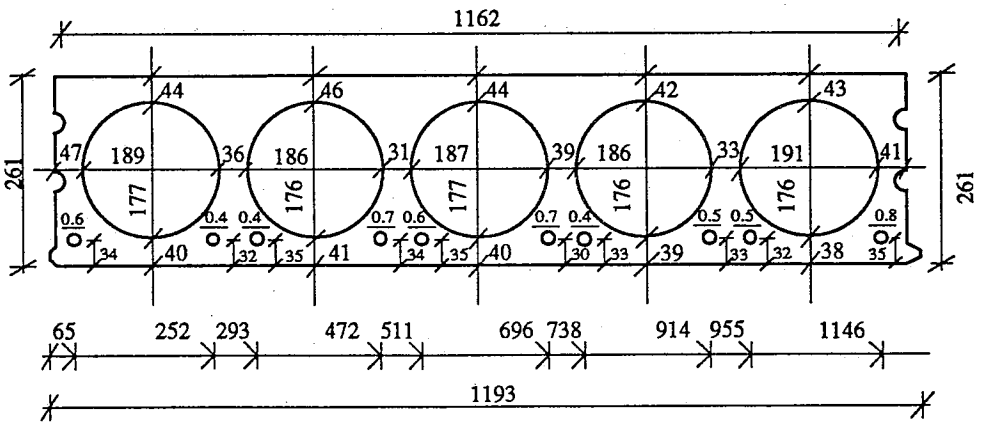

APPENDIX 3

8/10

GEOMETRY OF SLAB NO 8

STRAND: 10 ø 12.5
STRESS: 950 N/mm^2

LENGTH: 6010 mm
WEIGHT: 2560 kg

END 1 / EDGE 1

END 1 / EDGE 2

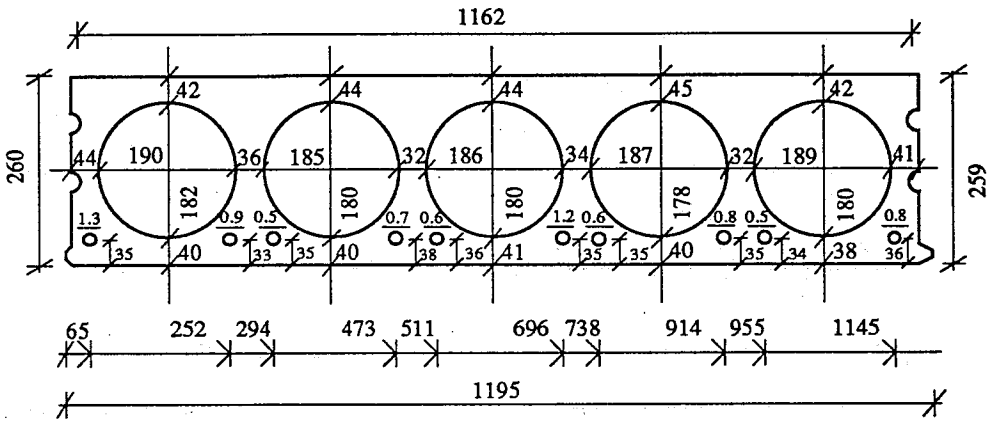

END 2 / EDGE 1

END 2 / EDGE 2

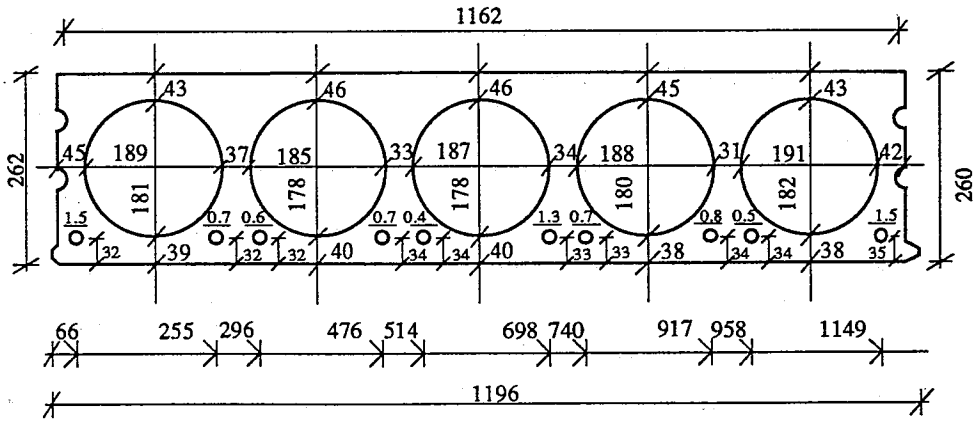

APPENDIX 3

9/10

GEOMETRY OF SLAB NO 9

STRAND: 10 ø 12,5
STRESS: 950 N/mm^2

LENGTH: 6000 mm
WEIGHT: 2560 kg

END 1 / EDGE 1

END 1 / EDGE 2

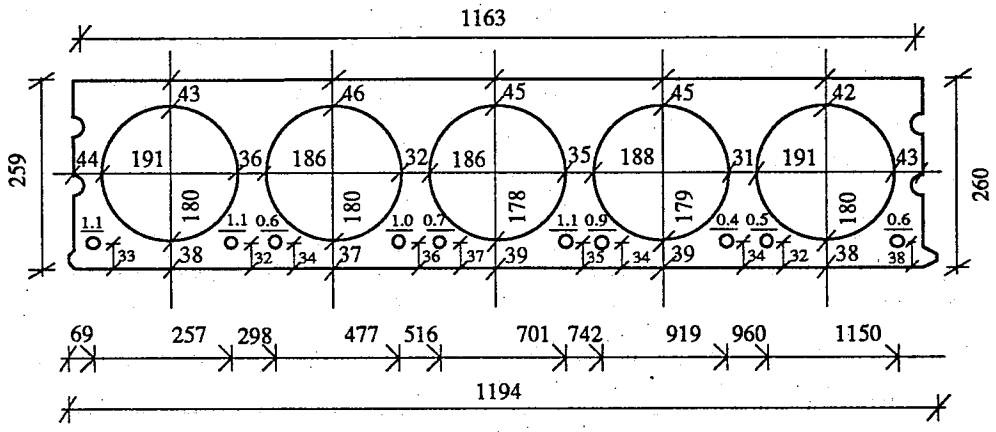

END 2 / EDGE 1

END 2 / EDGE 2

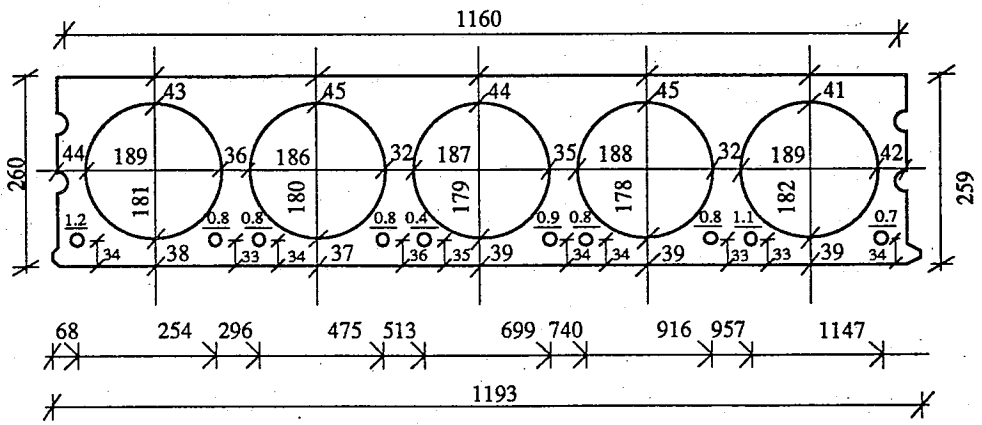

APPENDIX 3
10/10

GEOMETRY OF SLAB NO 10

STRAND: 10 ø 12,5
STRESS: 950 N/mm^2

LENGTH: 6000 mm
WEIGHT: 2510 kg

END 1 / EDGE 1

END 1 / EDGE 2

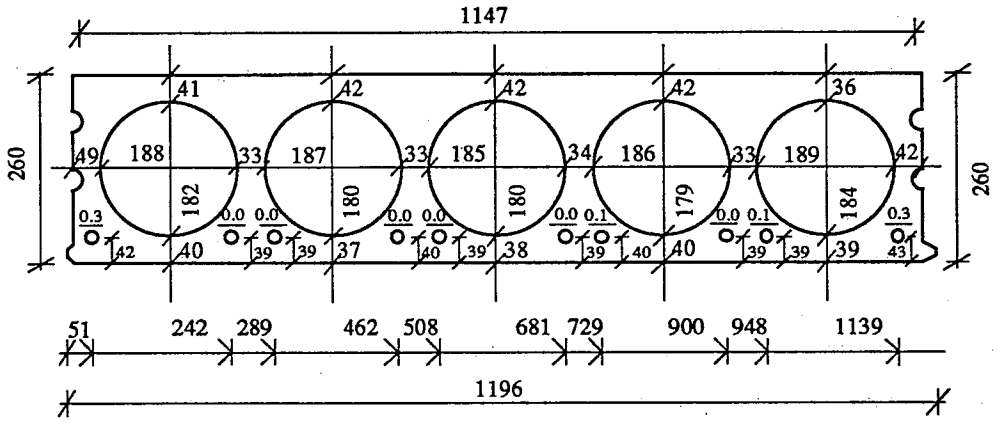

END 2 / EDGE 1

END 2 / EDGE 2

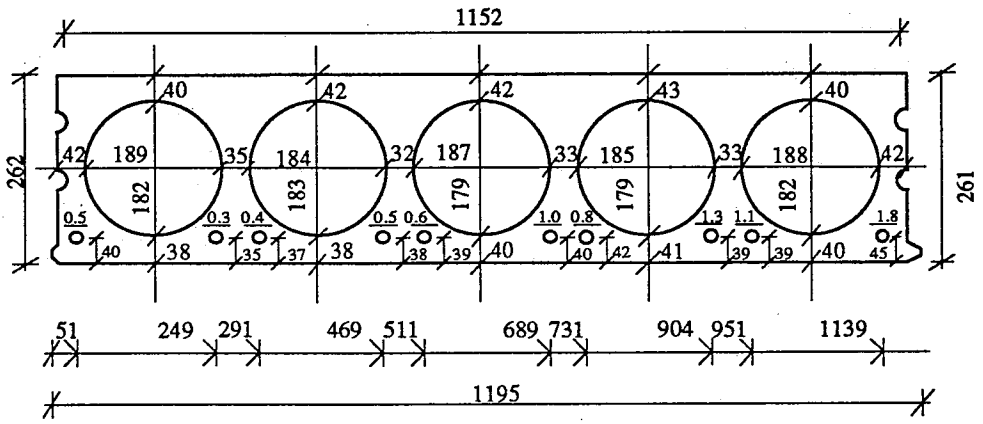

ELIMINATING RIGID BODY MOTION DUE TO YIELDING OF MIDDLE BEAM SUPPORTS FROM MEASURED DEFLECTION

1 DEFLECTION OF MIDDLE BEAM

The net deflection of beam (measured deflection - rigid body motion) at point x is obtained from

$$w_{x,o} = w_x - [(L_{beam}-x)w_1 + xw_2] / L_{beam}$$

where w_x, w_1 and w_2 denote the measured deflection at the distance of x from support 1, at support 1 and at support 2, respectively. L_{beam} denotes the span of the beam (cf. Fig. 1). The deflection due to the rigid body motion is obtained from

$$\Delta w_x = w_x - w_{x,0}$$

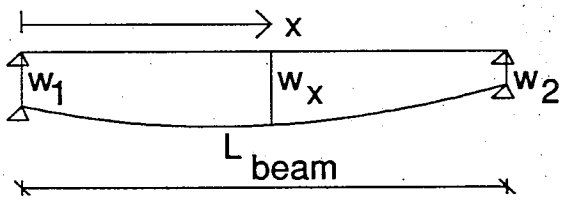

Fig. 1. Deflection of beam.

2 DEFLECTION OF SLAB

Due to technical difficulties, the yielding of the supports of the end beams was not measured. On the one hand, it is presumably quite small because the line load on the end beam is much lower than that on the middle beam. On the other hand, the yielding of the supports of the end beams is of minor importance when considering the shear failure close to the middle beam. For these reasons, this yielding is not taken into account when calculating the deflection of the slab.

The net deflection (measured deflection - rigid body motion) at point (x,y) of the slab is obtained from

$$w_{x,y,o} = w_{x,y} - (L_{slab}-y)\Delta w_{x,o} / L_{slab}$$

$w_{x,y}$ denotes the measured deflection at the point (x,y), $\Delta w_{x,o}$ the deflection due to the rigid body motion at support 1 of the slab (middle beam), and y is the distance of point (x,y) from support 1(middle beam). L_{slab} denotes the span of the slab (cf. Fig. 2).

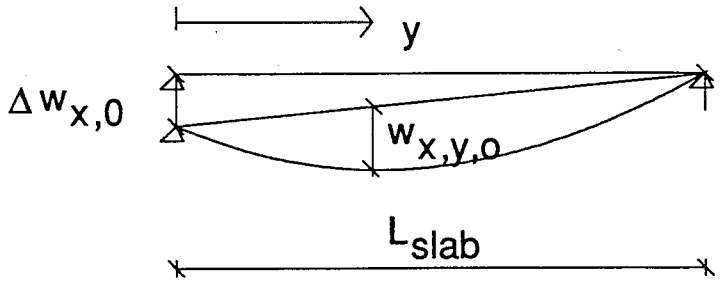

Fig. 2. Net deflection of slab.

FORCES AND DISPLACEMENTS IN THE FLOOR TEST

Table 1. Forces F_1, F_2 and forces in load cells no 2, 3 and 4.

F1 kN	F2 kN	2 kN	3 kN	4 kN
1,2	5,6	0	0	0
12,9	19,1	15,9	4,2	23,5
27,3	31	33	11,6	43,6
40,7	44,8	52,3	19,9	64,1
56,2	61,3	75,4	31,5	86,5
40	44,9	54,2	22,1	68,3
26,4	32,5	34,6	13,8	46,7
12,9	18	15	6,2	22,4
1,1	5,7	-0,5	1,8	-1,6
56,8	60,6	74,3	31,5	87,4
1,2	5,9	-0,4	1,9	-1,7
56,5	61,2	75,8	31,9	86,6
1,3	5,8	0,7	2,2	-1,3
56,9	61,5	76,9	32,3	86
1,3	5,6	0,9	2,2	-2,5
56,5	60,5	76,9	32,1	84,4
1,2	5,9	1,2	2,3	-3,2
14,7	19,1	18,3	6,9	21,9
28,1	32,3	36,6	14,2	43
41,1	44,8	54,4	21,6	62
56,4	61,3	78	32,7	84
61,3	66	85,2	36,3	90,3
66,2	70,9	92,5	39,9	96,8
71,5	76,1	100	44,4	103,3
76,6	79,9	106,8	47,9	109,3
81,3	85,5	113,4	52,1	115,9
86,5	90,3	118,4	55,6	124,3
92,2	95,8	125,5	59,8	132,5
96,6	100,9	132,3	63,9	139,5
101,3	105,6	138,5	67,5	145,9
106,4	110,9	145,9	71,9	152,8
111,5	114,9	153,5	74,6	157,9
116,7	121	163	78,4	165,4
121,9	126	172,5	82,7	169,5
121,5	124,8	172,6	81,9	166,6
121,4	124,4	174,2	80,3	165,5
123,4	127,2	178,8	82,3	169,1
125,6	129,4	182,4	83,7	171,8
126,4	130,8	184,4	84,3	173
128,8	132,4	189,5	85,2	174,3

130,4	133,7	191,9	86,3	176
131,8	136,1	196	87,1	178
133,5	138	201,6	87	179,1
135,2	139,9	205,6	87,4	180,9
136,6	141,8	209,5	87,7	182,4
136,8	134,7	207,5	85,8	182,1
136,9	129,6	205,4	82,2	179
136,8	129,2	203	79,7	176,2
136,1	137,5	212,3	83,9	182,7
136,1	141,3	221,2	83,8	185,1
136,4	132,4	227,7	72,8	162,6

Table 2. Deflection measured by transducers no 5, 6, 7, 8, 9, 10, 11, 12, 13 and 14.

F2 kN	5 mm	6 mm	7 mm	8 mm	9 mm	10 mm	11 mm	12 mm	13 mm	14 mm
5,6	0	0	0	0	0	0	0	0	0	0
19,1	0,031	0,08	0,08	0,07	0,043	0,29	0,37	0,38	0,39	0,35
31	0,067	0,17	0,2	0,17	0,095	0,62	0,77	0,85	0,82	0,71
44,8	0,125	0,38	0,56	0,39	0,169	0,98	1,31	1,58	1,39	1,1
61,3	0,235	0,81	1,3	0,82	0,287	1,49	2,1	2,71	2,22	1,61
44,9	0,216	0,83	1,4	0,85	0,264	1,22	1,85	2,47	1,95	1,34
32,5	0,169	0,73	1,26	0,75	0,213	0,85	1,43	1,99	1,5	0,95
18	0,12	0,63	1,09	0,62	0,155	0,46	0,97	1,42	0,98	0,51
5,7	0,073	0,5	0,93	0,52	0,095	0,08	0,51	0,88	0,51	0,13
60,6	0,252	0,94	1,56	0,95	0,305	1,49	2,25	2,95	2,36	1,63
5,9	0,084	0,56	1,03	0,56	0,104	0,09	0,54	0,94	0,54	0,12
61,2	0,274	1,03	1,74	1,05	0,325	1,52	2,3	3,07	2,42	1,65
5,8	0,092	0,6	1,11	0,6	0,114	0,11	0,61	1,01	0,58	0,13
61,5	0,28	1,09	1,82	1,1	0,329	1,52	2,35	3,15	2,47	1,67
5,6	0,091	0,6	1,15	0,61	0,115	0,09	0,61	1,04	0,58	0,13
60,5	0,282	1,1	1,84	1,12	0,332	1,52	2,36	3,18	2,48	1,66
5,9	0,092	0,63	1,15	0,62	0,116	0,09	0,59	1,04	0,59	0,13
19,1	0,13	0,73	1,29	0,72	0,164	0,4	0,99	1,53	1,02	0,49
32,3	0,176	0,83	1,47	0,85	0,224	0,78	1,44	2,09	1,51	0,88
44,8	0,225	0,96	1,65	0,97	0,277	1,14	1,87	2,62	1,97	1,26
61,3	0,286	1,12	1,88	1,13	0,34	1,52	2,39	3,23	2,51	1,66
66	0,309	1,19	2,01	1,22	0,361	1,67	2,55	3,48	2,71	1,81
70,9	0,336	1,32	2,21	1,32	0,393	1,79	2,77	3,77	2,92	1,94
76,1	0,371	1,45	2,47	1,5	0,431	1,94	3,02	4,15	3,2	2,09
79,9	0,405	1,62	2,77	1,65	0,467	2,09	3,28	4,54	3,48	2,25
85,5	0,454	1,83	3,15	1,88	0,523	2,29	3,63	5,07	3,85	2,48
90,3	0,51	2,1	3,61	2,15	0,587	2,51	4,03	5,69	4,3	2,7
95,8	0,566	2,34	4,05	2,4	0,645	2,74	4,45	6,31	4,75	2,95
100,9	0,61	2,52	4,36	2,59	0,685	2,92	4,78	6,76	5,07	3,15
105,6	0,658	2,73	4,76	2,81	0,733	3,12	5,12	7,29	5,45	3,33
110,9	0,715	2,98	5,2	3,07	0,785	3,35	5,56	7,94	5,89	3,55
114,9	0,792	3,34	5,84	3,45	0,852	3,63	6,11	8,8	6,49	3,81
121	0,892	3,83	6,72	3,96	0,943	4,04	6,89	10,03	7,31	4,18
126	1,008	4,4	7,74	4,54	1,059	4,51	7,83	11,51	8,3	4,68
124,8	1,026	4,52	7,98	4,68	1,081	4,6	8,04	11,86	8,54	4,82
124,4	1,043	4,62	8,13	4,77	1,102	4,69	8,22	12,13	8,74	4,91
127,2	1,062	4,69	8,28	4,87	1,123	4,78	8,37	12,36	8,9	5,01
129,4	1,084	4,8	8,46	4,97	1,141	4,87	8,56	12,61	9,07	5,11
130,8	1,1	4,88	8,6	5,04	1,155	4,94	8,67	12,81	9,21	5,18
132,4	1,141	5,09	9	5,28	1,201	5,15	9,09	13,42	9,65	5,4

APPENDIX 5

4/16

133,7	1,158	5,18	9,15	5,36	1,217	5,21	9,21	13,65	9,8	5,48
136,1	1,195	5,35	9,47	5,55	1,251	5,36	9,51	14,11	10,12	5,65
138	1,237	5,58	9,87	5,78	1,294	5,6	9,94	14,76	10,57	5,89
139,9	1,27	5,72	10,14	5,94	1,327	5,73	10,21	15,17	10,86	6,05
141,8	1,295	5,86	10,4	6,08	1,353	5,87	10,47	15,58	11,15	6,2
134,7	1,244	5,82	10,35	6,08	1,388	5,85	10,54	15,78	11,45	6,69
129,6	1,23	5,81	10,36	6,07	1,392	5,86	10,57	15,85	11,52	6,77
129,2	1,214	5,82	10,36	6,08	1,405	5,81	10,58	15,92	11,62	6,89
137,5	1,207	5,91	10,51	6,18	1,457	6	10,94	16,45	12,16	7,42
141,3	1,198	6,08	10,83	6,38	1,541	6,22	11,48	17,32	13	8,22
132,4	1,248	6,12	10,86	6,38	1,504	7,19	12,3	18,04	13,56	8,62

Table 3. Deflections measured by transducers no 15, 16, 17, 18 and 19.

F2 kN	15 mm	16 mm	17 mm	18 mm	19 mm
5,6	0	0	0	0	0
19,1	0,12	0,36	0,45	0,41	0,162
31	0,214	0,75	0,98	0,82	0,301
44,8	0,305	1,23	1,61	1,32	0,423
61,3	0,405	1,87	2,47	2	0,552
44,9	0,344	1,62	2,14	1,73	0,506
32,5	0,273	1,25	1,66	1,35	0,414
18	0,179	0,82	1,1	0,9	0,274
5,7	0,056	0,42	0,59	0,46	0,13
60,6	0,407	1,98	2,63	2,12	0,584
5,9	0,06	0,44	0,63	0,5	0,152
61,2	0,411	2,04	2,71	2,18	0,603
5,8	0,069	0,49	0,71	0,57	0,171
61,5	0,415	2,07	2,74	2,24	0,618
5,6	0,069	0,5	0,73	0,58	0,171
60,5	0,415	2,08	2,78	2,24	0,622
5,9	0,072	0,51	0,72	0,58	0,178
19,1	0,195	0,91	1,23	1,01	0,326
32,3	0,278	1,32	1,75	1,44	0,453
44,8	0,344	1,68	2,22	1,82	0,542
61,3	0,419	2,11	2,8	2,27	0,631
66	0,44	2,26	3	2,46	0,661
70,9	0,466	2,44	3,24	2,62	0,692
76,1	0,495	2,64	3,52	2,84	0,727
79,9	0,52	2,86	3,83	3,07	0,76
85,5	0,545	3,1	4,17	3,33	0,798
90,3	0,569	3,39	4,62	3,64	0,821
95,8	0,596	3,75	5,14	4,01	0,863
100,9	0,616	4,03	5,54	4,3	0,893
105,6	0,638	4,35	6,01	4,63	0,916
110,9	0,663	4,72	6,6	5,03	0,948
114,9	0,677	5,31	7,46	5,61	0,975
121	0,708	6,11	8,69	6,42	1,016
126	0,729	7,03	10,18	7,48	1,033
124,8	0,727	7,29	10,62	7,83	1,033
124,4	0,69	7,52	10,95	8,06	1,033
127,2	0,702	7,67	11,16	8,22	1,045
129,4	0,711	7,83	11,43	8,41	1,051
130,8	0,717	7,97	11,65	8,56	1,055
132,4	0,731	8,42	12,34	9,06	1,068

133,7	0,737	8,58	12,57	9,21	1,069
136,1	0,745	8,89	13,09	9,57	1,077
138	0,753	9,36	13,84	10,11	1,088
139,9	0,759	9,65	14,3	10,4	1,095
141,8	0,767	9,93	14,77	10,73	1,103
134,7	0,767	10,14	15,2	11,04	1,083
129,6	0,76	10,25	15,37	11,11	1,085
129,2	0,754	10,34	15,55	11,22	1,076
137,5	0,77	10,81	16,34	11,79	1,093
141,3	0,782	11,64	17,68	12,7	1,097
132,4	0,764	12,59	19,15	13,47	1,099

Table 4. Deflections measured by transducers no 20, 21, 22, 23, 24, 25, 26, 27, 28 and 29.

F2 kN	20 mm	21 mm	22 mm	23 mm	24 mm	25 mm	26 mm	27 mm	28 mm	29 mm
5,6	0	0	0	0	0	0	0	0	0	0
19,1	0,32	0,34	0,36	0,37	0,31	0,028	0,07	0,35	0,07	0,033
31	0,63	0,72	0,78	0,76	0,64	0,065	0,13	0,47	0,14	0,072
44,8	1	1,2	1,35	1,28	1,05	0,112	0,24	0,69	0,26	0,12
61,3	1,5	1,97	2,41	2,09	1,48	0,211	0,64	1,41	0,71	0,226
44,9	1,22	1,72	2,18	1,85	1,23	0,195	0,67	1,42	0,73	0,207
32,5	0,87	1,3	1,73	1,42	0,87	0,153	0,57	1,31	0,64	0,164
18	0,47	0,83	1,21	0,93	0,48	0,104	0,48	1,19	0,54	0,121
5,7	0,1	0,41	0,75	0,5	0,11	0,063	0,37	1,06	0,44	0,075
60,6	1,52	2,09	2,61	2,23	1,52	0,23	0,76	1,55	0,82	0,239
5,9	0,1	0,43	0,79	0,52	0,11	0,065	0,4	1,11	0,48	0,078
61,2	1,56	2,14	2,67	2,28	1,54	0,231	0,77	1,6	0,85	0,244
5,8	0,12	0,47	0,85	0,56	0,13	0,07	0,42	1,14	0,5	0,085
61,5	1,56	2,17	2,73	2,32	1,55	0,238	0,79	1,64	0,89	0,249
5,6	0,12	0,49	0,87	0,56	0,13	0,072	0,44	1,17	0,52	0,086
60,5	1,57	2,17	2,75	2,33	1,54	0,243	0,81	1,66	0,89	0,251
5,9	0,11	0,48	0,88	0,57	0,12	0,072	0,44	1,19	0,53	0,087
19,1	0,45	0,88	1,32	1	0,47	0,109	0,52	1,29	0,61	0,129
32,3	0,81	1,31	1,81	1,44	0,83	0,157	0,62	1,41	0,7	0,171
44,8	1,17	1,72	2,27	1,88	1,18	0,198	0,71	1,54	0,79	0,211
61,3	1,59	2,21	2,8	2,36	1,55	0,243	0,82	1,69	0,91	0,253
66	1,72	2,37	3	2,54	1,68	0,263	0,87	1,77	0,97	0,272
70,9	1,85	2,58	3,26	2,74	1,8	0,293	0,99	1,93	1,07	0,298
76,1	2	2,84	3,64	3,02	1,93	0,329	1,14	2,26	1,24	0,333
79,9	2,14	3,11	4,06	3,31	2,04	0,369	1,33	2,62	1,46	0,375
85,5	2,31	3,46	4,58	3,69	2,25	0,419	1,56	3,06	1,72	0,428
90,3	2,52	3,85	5,22	4,13	2,46	0,479	1,81	3,65	2	0,497
95,8	2,74	4,27	5,86	4,59	2,67	0,534	2,08	4,03	2,3	0,56
100,9	2,91	4,57	6,31	4,92	2,83	0,57	2,26	4,35	2,51	0,604
105,6	3,07	4,92	6,85	5,3	3,01	0,619	2,47	4,75	2,75	0,656
110,9	3,29	5,36	7,51	5,77	3,24	0,673	2,76	5,24	2,98	0,725
114,9	3,57	5,93	8,39	6,36	3,46	0,744	3,11	5,87	2,98	0,793
121	3,95	6,71	9,6	7,18	3,8	0,83	3,58	6,82	2,98	0,897
126	4,41	7,61	11,03	8,2	4,29	0,343	4,09	8,08	2,98	1,102
124,8	4,5	7,83	11,38	8,47	4,44	0,36	4,21	8,32	2,98	1,132
124,4	4,62	8,01	11,64	8,67	4,56	0,379	4,28	8,45	2,99	1,148
127,2	4,71	8,16	11,84	8,82	4,65	0,396	4,35	8,56	2,99	1,168
129,4	4,82	8,33	12,08	9	4,74	0,413	4,45	8,73	2,98	1,186
130,8	4,89	8,45	12,27	9,14	4,83	0,429	4,51	8,85	2,98	1,201

APPENDIX 5

8/16

132,4	5,11	8,85	12,87	9,58	5,05	0,469	4,73	9,25	2,98	1,248
133,7	5,2	8,99	13,1	9,74	5,13	0,488	4,81	9,42	2,99	1,267
136,1	5,34	9,28	13,55	10,07	5,29	0,52	4,98	9,72	2,98	1,305
138	5,58	9,7	14,16	10,52	5,55	0,549	5,16	10,08	2,98	1,352
139,9	5,75	9,96	14,56	10,79	5,69	0,571	5,29	10,31	2,98	1,381
141,8	5,87	10,22	14,94	11,08	5,86	0,593	5,42	10,53	2,98	1,405
134,7	5,9	10,36	15,17	11,22	5,89	0,598	5,5	10,67	2,98	1,407
129,6	5,98	10,44	15,25	11,27	5,91	0,598	5,5	10,68	2,99	1,4
129,2	5,99	10,48	15,33	11,36	5,98	0,59	5,51	10,69	2,98	1,403
137,5	6,21	10,83	15,85	11,91	6,59	0,584	5,58	10,82	2,98	1,458
141,3	6,63	11,45	16,71	12,7	7,27	0,594	5,74	11,14	2,98	1,524
132,4	7,22	12,12	17,49	13,25	7,55	0,61	5,88	11,44	2,99	1,529

Table 5. Horizontal displacement differences measured by transducers no 40, 41, 42, 43, 44 and 45.

F2 kN	40 mm	41 mm	42 mm	43 mm	44 mm	45 mm
5,6	0	0	0	0	0	0
19,1	0,008	0,002	-0,006	0	0,004	0,007
31	0,025	0,006	-0,003	0	0,013	0,015
44,8	0,056	0,01	0,008	0,004	0,039	0,028
61,3	0,094	0,012	0,022	0,013	0,074	0,048
44,9	0,088	0,011	0,019	0,014	0,069	0,047
32,5	0,066	0,007	0,016	0,014	0,047	0,039
18	0,04	0,002	0,012	0,014	0,026	0,028
5,7	0,02	-0,001	0,007	0,012	0,012	0,017
60,6	0,101	0,013	0,026	0,015	0,08	0,051
5,9	0,021	-0,001	0,003	0,012	0,013	0,018
61,2	0,105	0,012	0,027	0,016	0,083	0,051
5,8	0,023	-0,002	0,008	0,013	0,013	0,018
61,5	0,109	0,012	0,027	0,017	0,083	0,052
5,6	0,026	-0,003	0,008	0,014	0,014	0,018
60,5	0,11	0,012	0,026	0,017	0,083	0,053
5,9	0,027	-0,003	0,008	0,013	0,011	0,018
19,1	0,042	-0,002	0,011	0,014	0,018	0,025
32,3	0,065	0,002	0,01	0,014	0,037	0,034
44,8	0,092	0,006	0,017	0,016	0,06	0,043
61,3	0,113	0,012	0,03	0,017	0,086	0,052
66	0,118	0,013	0,034	0,019	0,096	0,056
70,9	0,128	0,015	0,045	0,02	0,103	0,059
76,1	0,137	0,017	0,058	0,022	0,115	0,062
79,9	0,145	0,018	0,083	0,026	0,121	0,067
85,5	0,178	0,02	0,16	0,03	0,137	0,072
90,3	0,257	0,013	0,235	0,029	0,162	0,087
95,8	0,341	0	0,296	0,03	0,196	0,072
100,9	0,377	-0,002	0,329	0,03	0,22	0,071
105,6	0,422	-0,005	0,37	0,029	0,265	0,072
110,9	0,483	-0,007	0,417	0,029	0,328	0,075
114,9	0,548	-0,01	0,462	0,034	0,448	0,078
121	0,651	-0,026	0,477	0,142	0,591	0,086
126	0,781	0,067	0,485	0,275	0,695	0,093
124,8	0,773	0,17	0,482	0,302	0,699	0,096
124,4	0,766	0,21	0,488	0,317	0,677	0,1
127,2	0,77	0,218	0,485	0,324	0,675	0,101
129,4	0,773	0,231	0,496	0,334	0,681	0,101
130,8	0,775	0,245	0,498	0,341	0,681	0,102

132,4	0,785	0,277	0,506	0,364	0,684	0,104
133,7	0,787	0,287	0,511	0,371	0,686	0,104
136,1	0,797	0,311	0,516	0,386	0,69	0,105
138	0,81	0,355	0,52	0,411	0,689	0,107
139,9	0,821	0,379	0,528	0,425	0,688	0,109
141,8	0,831	0,409	0,54	0,441	0,688	0,113
134,7	0,828	0,422	0,556	0,446	0,691	0,112
129,6	0,824	0,445	0,557	0,45	0,668	0,11
129,2	0,816	0,48	0,557	0,453	0,66	0,109
137,5	0,799	0,6	0,584	0,475	0,658	0,108
141,3	0,905	0,668	0,638	0,51	0,646	0,104
132,4	0,916	0,638	0,675	0,526	0,65	0,183

Table 6. Displacement differences on the surface of the topping measured by transducers 50, 51, 52, 53, 54 and 55.

F2 kN	50 mm	51 mm	52 mm	53 mm	54 mm	55 mm
5,6	0	0	0	0	0	0
19,1	-0,024	-0,025	-0,028	-0,024	-0,025	-0,024
31	-0,053	-0,056	-0,057	-0,052	-0,054	-0,052
44,8	-0,089	-0,096	-0,098	-0,091	-0,091	-0,087
61,3	-0,139	-0,154	-0,157	-0,148	-0,144	-0,14
44,9	-0,119	-0,132	-0,138	-0,129	-0,127	-0,12
32,5	-0,089	-0,101	-0,105	-0,099	-0,1	-0,092
18	-0,058	-0,069	-0,07	-0,067	-0,067	-0,062
5,7	-0,03	-0,039	-0,039	-0,037	-0,039	-0,034
60,6	-0,147	-0,167	-0,17	-0,16	-0,154	-0,149
5,9	-0,032	-0,042	-0,042	-0,041	-0,04	-0,037
61,2	-0,151	-0,171	-0,174	-0,164	-0,159	-0,154
5,8	-0,034	-0,044	-0,045	-0,044	-0,044	-0,04
61,5	-0,153	-0,173	-0,179	-0,168	-0,161	-0,157
5,6	-0,035	-0,047	-0,048	-0,045	-0,046	-0,041
60,5	-0,154	-0,173	-0,18	-0,169	-0,162	-0,158
5,9	-0,036	-0,048	-0,048	-0,046	-0,045	-0,043
19,1	-0,062	-0,074	-0,078	-0,073	-0,072	-0,068
32,3	-0,092	-0,108	-0,112	-0,106	-0,101	-0,098
44,8	-0,121	-0,14	-0,144	-0,136	-0,13	-0,127
61,3	-0,156	-0,178	-0,183	-0,172	-0,165	-0,161
66	-0,168	-0,191	-0,196	-0,185	-0,177	-0,174
70,9	-0,182	-0,208	-0,212	-0,199	-0,192	-0,188
76,1	-0,2	-0,225	-0,233	-0,218	-0,211	-0,206
79,9	-0,218	-0,247	-0,254	-0,238	-0,23	-0,225
85,5	-0,232	-0,262	-0,281	-0,264	-0,256	-0,249
90,3	-0,244	-0,283	-0,313	-0,282	-0,286	-0,279
95,8	-0,262	-0,302	-0,339	-0,305	-0,319	-0,309
100,9	-0,278	-0,322	-0,361	-0,325	-0,34	-0,332
105,6	-0,294	-0,34	-0,384	-0,348	-0,366	-0,358
110,9	-0,313	-0,365	-0,412	-0,375	-0,397	-0,388
114,9	-0,34	-0,399	-0,445	-0,409	-0,435	-0,428
121	-0,388	-0,442	-0,494	-0,445	-0,478	-0,472
126	-0,435	-0,504	-0,522	-0,468	-0,518	-0,521
124,8	-0,448	-0,529	-0,526	-0,474	-0,523	-0,538
124,4	-0,459	-0,546	-0,533	-0,482	-0,531	-0,552
127,2	-0,468	-0,554	-0,542	-0,49	-0,54	-0,563
129,4	-0,478	-0,568	-0,553	-0,5	-0,553	-0,575
130,8	-0,486	-0,578	-0,56	-0,506	-0,56	-0,585

132,4	-0,516	-0,617	-0,582	-0,527	-0,583	-0,621
133,7	-0,525	-0,629	-0,589	-0,535	-0,593	-0,633
136,1	-0,545	-0,659	-0,606	-0,551	-0,612	-0,659
138	-0,576	-0,711	-0,631	-0,574	-0,638	-0,702
139,9	-0,595	-0,739	-0,649	-0,589	-0,655	-0,729
141,8	-0,614	-0,766	-0,664	-0,603	-0,673	-0,757
134,7	-0,624	-0,808	-0,663	-0,625	-0,671	-0,795
129,6	-0,631	-0,818	-0,668	-0,63	-0,675	-0,806
129,2	-0,637	-0,836	-0,667	-0,637	-0,679	-0,818
137,5	-0,651	-0,894	-0,677	-0,671	-0,693	-0,861
141,3	-0,687	-0,969	-0,701	-0,713	-0,724	-0,897
132,4	-0,786	-1,011	-0,774	-0,729	-0,853	-0,91

APPENDIX 5

Table 7. Displacement differencies on the bottom of the slab units and the middle beam measured by transducers 56, 57, 58, 59, 60 and 61.

F2 kN	56 mm	57 mm	58 mm	59 mm	60 mm	61 mm
5,6	0	0	0	0	0	0
19,1	0,013	0,005	0,028	0,019	0,019	0,017
31	0,032	0,021	0,07	0,061	0,04	0,036
44,8	0,059	0,052	0,129	0,117	0,066	0,066
61,3	0,078	0,07	0,216	0,199	0,097	0,099
44,9	0,059	0,045	0,187	0,17	0,08	0,082
32,5	0,039	0,024	0,142	0,126	0,061	0,065
18	0,017	0	0,095	0,085	0,035	0,039
5,7	-0,002	-0,015	0,054	0,046	0,017	0,021
60,6	0,073	0,059	0,229	0,213	0,099	0,102
5,9	-0,001	-0,019	0,054	0,046	0,02	0,025
61,2	0,077	0,056	0,234	0,215	0,104	0,107
5,8	-0,001	-0,018	0,057	0,049	0,021	0,024
61,5	0,077	0,054	0,237	0,22	0,102	0,105
5,6	-0,003	-0,019	0,056	0,048	0,021	0,024
60,5	0,073	0,056	0,237	0,22	0,102	0,105
5,9	-0,004	-0,021	0,057	0,046	0,023	0,031
19,1	0,013	-0,006	0,097	0,086	0,039	0,047
32,3	0,032	0,013	0,142	0,129	0,058	0,065
44,8	0,048	0,032	0,186	0,172	0,077	0,085
61,3	0,074	0,055	0,239	0,222	0,102	0,11
66	0,081	0,063	0,259	0,24	0,112	0,12
70,9	0,088	0,072	0,282	0,261	0,121	0,128
76,1	0,098	0,083	0,314	0,293	0,133	0,14
79,9	0,109	0,095	0,348	0,326	0,144	0,152
85,5	0,124	0,109	0,388	0,361	0,16	0,171
90,3	0,142	0,129	0,436	0,407	0,183	0,193
95,8	0,162	0,153	0,495	0,461	0,205	0,213
100,9	0,177	0,168	0,542	0,497	0,223	0,231
105,6	0,189	0,182	0,617	0,537	0,242	0,252
110,9	0,201	0,199	0,751	0,588	0,265	0,277
114,9	0,22	0,227	0,907	0,654	0,309	0,316
121	0,282	0,287	1,085	0,759	0,411	0,381
126	0,46	0,454	1,245	0,924	0,512	0,547
124,8	0,503	0,501	1,271	0,978	0,541	0,617
124,4	0,532	0,536	1,296	1,014	0,559	0,646
127,2	0,546	0,553	1,323	1,037	0,572	0,662
129,4	0,546	0,574	1,354	1,069	0,588	0,687
130,8	0,563	0,594	1,379	1,097	0,601	0,704

132,4	0,619	0,677	1,455	1,185	0,637	0,758
133,7	0,636	0,709	1,484	1,216	0,649	0,778
136,1	0,679	0,787	1,544	1,279	0,669	0,823
138	0,701	0,896	1,621	1,366	0,697	0,878
139,9	0,734	0,958	1,675	1,426	0,717	0,915
141,8	0,766	1,027	1,731	1,486	0,733	0,946
134,7	0,765	1,113	1,741	1,57	0,732	0,953
129,6	0,766	1,14	1,751	1,591	0,729	0,955
129,2	0,767	1,167	1,761	1,621	0,721	0,959
137,5	0,78	1,257	1,802	1,763	0,724	1
141,3	0,788	1,478	1,889	1,942	0,714	1,043
132,4	0,824	1,527	2,123	2,033	0,654	1,028

Table 8. Displacement differencies between the ends of the middle beam and the slab edges measured by transducers 46, 47, 48, 49, 62, 61 64 and 65.

F2 kN	46 mm	47 mm	48 mm	49 mm	62 mm	63 mm	64 mm	65 mm
5,6	0	0	0	0	0	0	0	0
19,1	0	0,01	0,001	0,001	0	0	0	0
31	0,01	0,02	-0,007	0	0,007	-0,001	0,002	0,001
44,8	0,01	0,02	-0,018	-0,003	0,011	-0,001	-0,001	0,001
61,3	0,01	0,03	-0,033	-0,012	0,012	0	-0,017	0,003
44,9	0,04	0,04	-0,036	-0,026	0,014	-0,001	-0,02	0,003
32,5	0,04	0,03	-0,034	-0,023	0,009	0	-0,02	0,002
18	0,04	0,02	-0,021	-0,017	0,005	-0,001	0,001	0,004
5,7	0,03	0	-0,009	-0,013	0,005	-0,001	0,005	0,003
60,6	0,04	0,03	-0,036	-0,024	0,011	-0,001	-0,012	0,003
5,9	0,03	0,01	-0,012	-0,013	0,003	0	0,005	0,001
61,2	0,04	0,03	-0,038	-0,025	0,011	0	-0,012	0,004
5,8	0,03	0,01	-0,014	-0,015	0,006	-0,001	0,002	0,001
61,5	0,04	0,03	-0,038	-0,026	0,009	-0,001	-0,013	0,003
5,6	0,04	0,01	-0,013	-0,015	0,002	-0,001	0,003	0,001
60,5	0,04	0,03	-0,043	-0,027	0,01	-0,001	-0,012	0,003
5,9	0,04	0,01	-0,014	-0,016	0,003	0,005	0,003	0
19,1	0,04	0,01	-0,013	-0,016	0,005	0,005	0,003	-0,001
32,3	0,04	0,02	-0,022	-0,021	0,009	0,004	0,001	0
44,8	0,04	0,02	-0,032	-0,023	0,009	0,004	-0,008	0,001
61,3	0,04	0,03	-0,04	-0,028	0,011	0,004	-0,013	0,003
66	0,05	0,04	-0,043	-0,03	0	0,004	-0,009	0,003
70,9	0,05	0,04	-0,046	-0,033	0,002	0,005	-0,01	0,002
76,1	0,05	0,05	-0,05	-0,036	0,003	0,005	-0,01	0,003
79,9	0,05	0,05	-0,054	-0,04	0,005	0,005	-0,012	0,003
85,5	0,06	0,05	-0,06	-0,045	0,004	0,007	-0,015	0,003
90,3	0,09	0,06	-0,075	-0,052	-0,006	0,007	-0,023	0,004
95,8	0,15	0,07	-0,104	-0,075	-0,016	0,008	-0,033	0,001
100,9	0,18	0,07	-0,121	-0,091	-0,02	0,009	-0,039	0,001
105,6	0,22	0,09	-0,15	-0,114	-0,05	0,01	-0,046	0,001
110,9	0,25	0,1	-0,194	-0,141	-0,041	0,011	-0,053	0,002
114,9	0,3	0,13	-0,281	-0,197	-0,049	0,012	-0,064	0,002
121	0,38	0,17	-0,395	-0,279	-0,065	0,005	-0,076	0,001
126	0,54	0,34	-0,508	-0,357	-0,094	0,008	-0,088	0,002
124,8	0,62	0,45	-0,548	-0,388	-0,1	-0,003	-0,092	0,002
124,4	0,67	0,5	-0,588	-0,416	-0,11	-0,008	-0,102	-0,001
127,2	0,68	0,51	-0,597	-0,423	-0,111	-0,01	-0,106	-0,001
129,4	0,69	0,53	-0,61	-0,431	-0,119	-0,011	-0,111	-0,001
130,8	0,71	0,55	-0,624	-0,439	-0,122	-0,012	-0,119	-0,001

132,4	0,78	0,62	-0,672	-0,479	-0,137	-0,018	-0,133	-0,002
133,7	0,79	0,64	-0,684	-0,487	-0,139	-0,018	-0,136	-0,002
136,1	0,83	0,68	-0,713	-0,509	-0,148	-0,021	-0,145	-0,002
138	0,91	0,76	-0,774	-0,562	-0,17	-0,03	-0,177	0,007
139,9	0,95	0,81	-0,803	-0,583	-0,183	-0,036	-0,211	0,011
141,8	1	0,86	-0,839	-0,609	-0,199	-0,044	-0,29	0,02
134,7	1,08	0,97	-0,861	-0,621	-0,216	-0,154	-0,389	0,024
129,6	1,11	1,02	-0,877	-0,631	-0,224	-0,161	-0,737	0,028
129,2	1,15	1,06	-0,89	-0,642	-0,239	-0,169	-0,869	0,032
137,5	1,26	1,23	-0,92	-0,66	-0,276	-0,194	-0,968	0,035
141,3	1,53	1,54	-0,987	-0,697	-0,323	-0,242	-1,453	0,043
132,4	1,7	1,73	-1,178	-0,953	-0,35	-0,268	-3,116	0